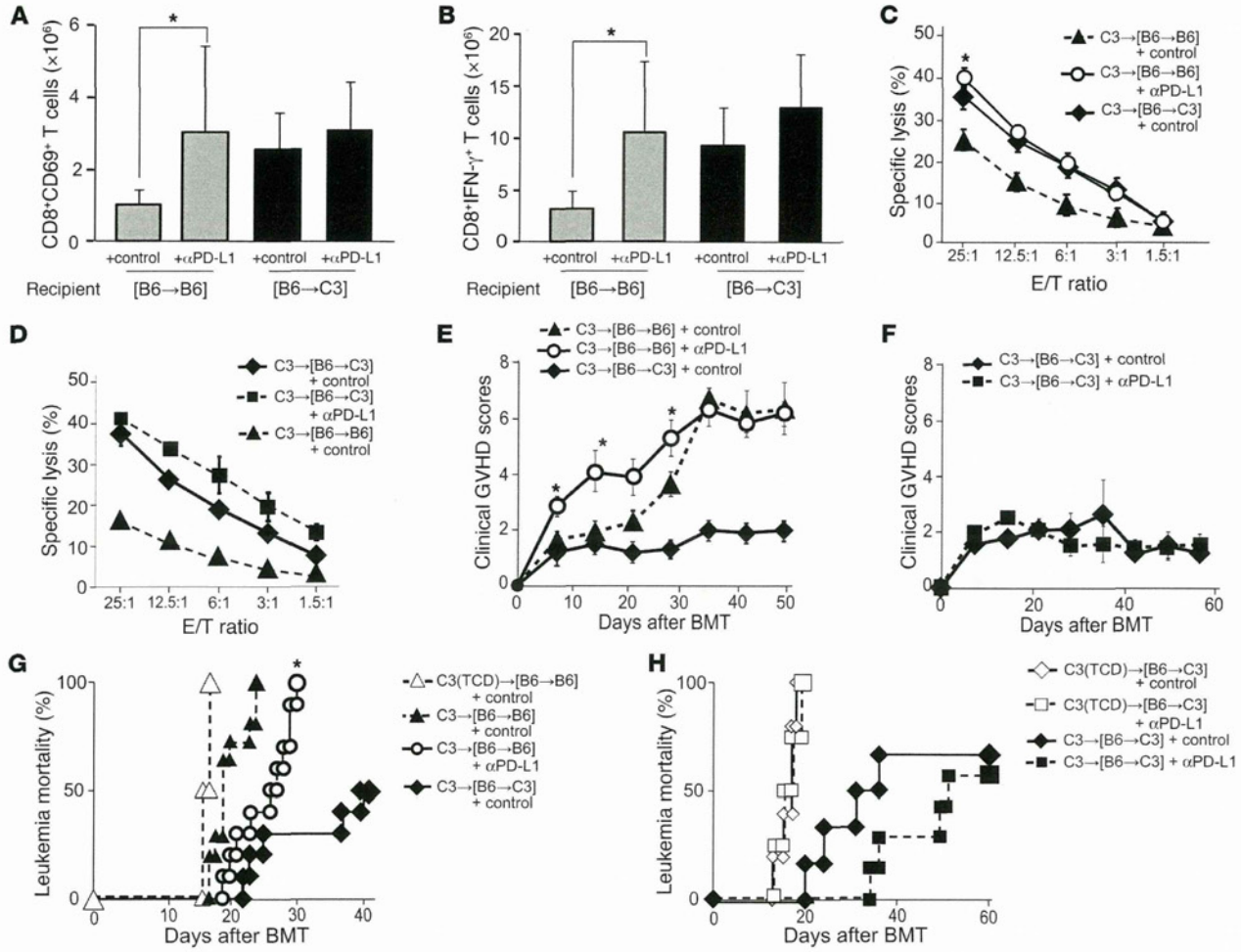

Figure 5

Blockade of the interaction between PD-1 and PD-L1 enhances GVL activity. [B6→C3] and [B6→B6] chimeras were reirradiated and injected with 5×10^6 TCD BM cells alone or with 1×10^6 $CD8^+$ T cells from C3 donors. Mice were i.p. injected with 500 μg of anti PD-L1 mAbs or controls on day 0 and then 200 μg thereafter on days +3, +6, +9, +12, +15, and +18. Splenocytes were harvested on day +14 to determine the number of $CD8^+CD69^+$ T cells (**A**) and IFN-γ–producing $CD8^+$ T cells (**B**) and CTL activity against EL4 targets (**C** and **D**). Results from a representative experiment of 2 similar experiments (means ± SD, n = 7–8/group). Mean clinical GVHD scores (±SEM) (**E** and **F**) after BMT are shown (n = 5–7/group). (**G** and **H**) Leukemia mortality after BMT in [B6→B6] and [B6→C3] chimeras injected with EL4 cells on day 0 (n = 4–11/group). Data from two similar experiments were combined. αPD-L1, anti–PD-L1 mAbs. *$P < 0.05$ compared with the corresponding controls.

tional tolerance of alloreactive, anti-donor $CD8^+$ T cells to achieve successful engraftment in BMT (42, 43). In this study, we found that PD-1 expression was upregulated in donor T cells and PD-L1 expression was upregulated in GVHD target organs. The expression of PD-1/PD-L1 was markedly reduced in chimeras lacking alloantigen expression on non-hematopoietic cells. PD-1 and PD-L1 expression is induced upon cell activation and inflammation in GVHD (44); therefore, the absence of alloantigen expression on GVHD target epithelium reduced GVHD in chimeric mice, which resulted in insufficient stimulation of the PD-1/PD-L1 interaction. Target tissue expression of PD-L1 is also critical for the induction of T cell exhaustion or tolerance in chronic viral infection, autoimmune diabetes, and cardiac allografting (19, 42, 45).

Both PD-1 and PD-L1 were markedly upregulated in [B6→B6] mice, but they were also modestly upregulated in [B6→C3] mice. Blockade of PD-1/PD-L1 interactions significantly restored T cell effector functions in [B6→B6] mice but modestly restored them in [B6→C3] mice as well. The relevance of these observations is shown by the PD-1/PD-L1 blockade studies. These data showed that the PD-1/PD-L1 pathway is particularly germane to [B6→B6] mice with widespread expression of alloantigens but also applies, at least in part, to [B6→C3] mice, wherein alloantigen expression is only on APCs. While there is likely to be a role for this pathway in the absence of epithelial alloantigen expression, the full negative impact of this pathway on GVL is only seen when alloantigen expression is present on non-hematopoietic tissues.

Of note, the improvement in GVL by the PD-1/PD-L1 blockade was partial, as has been shown in chronic viral infection (46–48). This may be due to the presence of multiple negative regulatory pathways that contribute to T cell exhaustion, including CTLA-4, IL-10, LAG-3, CD160, and 2B4 (20, 47, 49). In addition, the population of exhausted T cells is heterogeneous, and this interven-

tion is effective only for PD-1^{lo} and not PD-1^{hi}, which are subsets of exhausted T cells (50). Many of these inhibitory receptors are either coexpressed by the same exhausted T cells or differentially expressed on different subsets of exhausted cells. As the severity of the infection increases, the number of different inhibitors expressed per cell increases (47). A second inhibitory receptor, CTLA-4, can be overexpressed by exhausted CD4$^+$ T cells in chronic viral infection, but it appears to have a minimal role on exhausted CD8$^+$ T cells (19, 51). Although CTLA-4 was only slightly upregulated on CD8$^+$ T cells in contrast to the marked upregulation of PD-1 in our CD8-dependent model of MHC-matched BMT, the precise inhibitory receptors of therapeutic interest may differ between CD4$^+$-dependent and CD8$^+$-dependent GVHD/GVL. Another key negative regulatory pathway is mediated by Foxp3$^+$ Tregs. However, enhancement of GVL is not due to effects of the PD-1/PD-L1 blockade on Tregs, because blockade of PD-1/PD-L1 interactions enhances the expansion and function of Tregs (52). The hierarchy of these pathways in regulating GVL will need to be studied in the future based on better understanding of the delineation of T cell subsets and models (53). However, our results suggest the detrimental effect of GVHD-induced immunosuppression on GVL responses, regardless of which inhibitory pathway might be dominant clinically.

In addition, the administration of anti–PD-L1 mAb also exacerbated acute GVHD, as has been shown in a previous study (54). Therefore, the beneficial effects of the PD-1/PD-L1 blockade may be offset by the exacerbation of GVHD. Effects of the inhibitory receptor blockade might depend on the magnitude or stage of donor T cell activation and the severity of GVHD; therefore, the timing and duration of the targeting may be important.

In clinical HSCT, alloantigens continue to be presented on MHC class I in non-hematopoietic cells throughout the lifetime of the transplant recipients. However, a substantial number of patients eventually develop tolerance after resolution of GVHD and often experience leukemia relapse. Although activation-induced apoptosis of alloreactive T cells has been proposed as an explanation of this paradox (55), studies monitoring GVHD-specific T cell clones indicate that host-reactive T cells are continuously present after allogeneic HSCT (56–58). Our results provide a logical explanation for this paradox. However, the process of exhaustion is unlikely to occur in patients not developing GVHD, because induction of T cell exhaustion requires antigen-specific activation of T cells and subsequent differentiation into effector T cells. In these patients, tolerance could be induced by other mechanisms, such as functional central and peripheral tolerance mechanisms. It is well known that GVL is not apparent in patients with high leukemia burden. Although leukemia cells used in the current study do not express PD-L1 (22, 59), leukemia cells expressing PD-L1 may also directly limit the GVL response in patients with high leukemia burden (22, 24, 25). However, such insights from animal models must be extrapolated with caution to clinical studies involving humans.

It has been assumed that T cell exhaustion is antigen specific in chronic viral infection. Bystander lysis of T cells has also been reported in the course of viral infections (60), but is of minimal significance because of its limited magnitude and because normal thymic function can replenish the peripheral T cell pool. In contrast, in GVHD, T cell exhaustion occurs after initial T cell activation and the subsequent development of GVHD. GVHD induces bystander apoptosis of non-host-reactive T cells. In addition, GVHD-mediated injury of the thymus and the secondary lymphoid organs inhibits full replenishment of the peripheral T cell pool (55). Thus, establishment of full immune competence probably requires the additional process of T cell reconstitution following T cell exhaustion.

In conclusion, our results indicated the significance of alloantigen expression on non-hematopoietic cells in GVL. Alloantigen expression on non-hematopoietic cells induces the apoptosis of donor T cells and the dysfunction of cytotoxic effector function, which leads to a reduction in GVL activity. T cell dysfunction was partially restored by blocking PD-1/PD-L1 interactions, which suggests that the therapeutic "tuning" of T cell responses via modulation of negative regulatory pathways represents a novel strategy for enhancing GVL. Our results in combination with those of previous studies (6, 7, 9, 10, 38, 39) provide a complete picture of the effect of alloantigen expression on host APCs, GVHD target epithelium, and tumor cells in allogeneic HSCT; alloantigen expression on host non-hematopoietic cells augments GVHD but suppresses GVL effects. This concept may provide an important framework for understanding the pathophysiology of GVHD and allow for the separation of GVHD and GVL.

Methods

Mice. Female C57BL/6 (B6, H-2^b, CD45.2$^+$), BALB/c (Ba, H-2^d), and DBA/2 (Db, H-2^d) mice were purchased from Charles River Japan. B6.Ly5.1 (H-2^b, CD45.1$^+$) and C3H.Sw (C3, H-2^b) mice were purchased from The Jackson Laboratory. B6-background β_2m-deficient mice ($\beta_2m^{-/-}$: B6.129-β_2-m^{tm1Jae}N12) were purchased from Taconic. The age of mice used ranged from 8 to 12 weeks. Mice were maintained in specific pathogen–free conditions and received normal chaw and hyperchlorinated drinking water for the first 3 weeks after BMT. All experiments involving animals were performed according to a protocol approved by the Institutional Animal Care and Research Advisory Committee of Okayama University and Kyushu University.

Generation of bone marrow chimera and induction of GVHD and GVL. Total body irradiation (TBI: X-ray) was split into 2 doses separated by 4 hours to minimize gastrointestinal toxicity. B6 and C3 mice received 10 Gy TBI, whereas Ba and Db mice received 8.5 Gy TBI. To create BM chimeras, lethally irradiated mice were intravenously injected with 5×10^6 TCD BM cells from donors. TCD was performed using anti-CD90 microbeads and AutoMACS (Miltenyi Biotec). Four months later, the chimeric mice were reirradiated and injected with 5×10^6 TCD BM cells plus various doses of CD8$^+$ T cells or 2×10^6 T cells. T cells and CD8$^+$ T cells were negatively isolated from splenocytes by using a T cell isolation kit and a CD8$^+$ T cell isolation kit (Miltenyi Biotec), respectively, and the AutoMACS. In the GVL experiments, EL4 (H-2^b) derived from a B6 mouse, P815 (H-2^d) derived from a Db mouse, and A20 (H-2^d) derived from a Ba mouse were intravenously injected into BMT recipients on day 0 of BMT. Anti–PD-L1 mAbs were purified from the hybridoma supernatant of clone MIH5 (61), which was a gift from Miyuki Azuma of Tokyo Medical and Dental University, Tokyo, Japan, and i.p. injected at a dose of 500 μg/mouse on day 0, followed by 200 μg/mouse on days +3, +6, +9, +12, +15, and +18 after BMT.

Assessment of GVHD and GVL effects. Survival after BMT was monitored daily, and the degree of clinical GVHD was assessed weekly by using a scoring system that sums changes in 5 clinical parameters: weight loss, posture, activity, fur texture, and skin integrity (maximum index, 10) as described previously (13). The cause of each death after BMT was determined by post mortem examination, and was either GVHD or tumor. The most striking leukemia-specific abnormality induced by EL4, P815, and A20 was macroscopic tumor nodules, marked hepatosplenomegaly, and lower limb paralysis (62). Leukemia death induced by EL4, P815, and A20 was therefore defined by the occurrence of hepatosplenomegaly, macroscopic tumor nodules in the liver

and/or spleen, or hind leg paralysis. GVHD death was defined as the absence of leukemia and by the presence of clinical signs of GVHD, assessed by using a clinical scoring system. Animals surviving beyond the observation period of BMT were sacrificed, and the spleen and liver were harvested for histological evaluation to determine leukemia-free survival.

Flow cytometric analysis. The mAbs used were FITC-, PE-, PerCP-, Cy5.5-, or APC-conjugated anti–mouse CD5.1, CD8, CD45.1, CD45.2, CD69, and PD-1 (BD Biosciences). Cells positive for 7-amino-actinomycin D (BD Biosciences) were excluded from the analysis. For the analysis of donor T cell apoptosis, the cells were stained with Annexin V (MBL). For intracellular IFN-γ staining, the splenocytes were incubated for 4 hours with leukocyte activation cocktail and BD GolgiPlug (BD Biosciences) at 37°C. Then, the cells underwent permeabilization with a BD Cytofix/Cytoperm solution (BD Biosciences) and were stained with FITC-conjugated anti–IFN-γ mAbs (BD Biosciences). For intracellular CTLA-4 staining, cells were stained with PE-conjugated anti–CTLA-4 mAbs (eBioscience). At least 5,000 live events were acquired for the analysis using a FACSCalibur flow cytometer (BD Biosciences).

CTL assay. Splenocytes were removed from chimeric recipients 14 days after BMT, and the mononuclear cells were then separated by density gradient centrifugation. The percentage of $CD8^+$ cells in this fraction was determined by flow cytometry, and counts were normalized for $CD8^+$ cell numbers. Tumor targets, 2×10^6 P815 or EL4, were labeled with 100 μCi of ^{51}Cr sodium salt (Amersham Biosciences) for 2 hours. After washing 3 times, the labeled targets were resuspended in 10% FCS in RPMI and plated at 10^4 cells per well in U-bottom plates (Corning-Costar Corp.). Allogeneic splenocyte preparations, as described above, were added to quadruplicate wells at varying effector-to-target ratios and incubated for 4 hours. Maximal and background release were determined by adding 1% SDS and media alone to the targets, respectively. ^{51}Cr activity in the supernatants collected 4 hours later was determined using a Wallac 1470 WIZARD Gamma Counter (Wallac Oy), and lysis was expressed as a percentage of maximum: percentage of specific lysis = 100 (sample count − background count/maximum count − background count).

Quantitative real-time PCR. Total RNA was isolated from the frozen liver using ISOGEN (Nippon Gene). cDNA was synthesized from 150 μg RNA using a QuantiTect Reverse Transcription Kit (QIAGEN). *Pdl1* mRNA levels were quantified by real-time PCR using the 7500 Real-Time PCR System (Applied Biosystems). TaqMan Universal PCR MasterMix, primers, and the fluorescent TaqMan probe specific for murine PD-L1 (Mm00452054-m1) and a house keeping gene, mGAPDH (Mm99999915-g1), were purchased from Applied Biosystems. The standard was obtained using RNA extracted from syngeneic controls.

Immunohistochemistry. For immunohistochemical analysis, isolated livers were frozen in Tissue-Tek (Sakura Finetek), and 5-μm cryostat sections were prepared. Slides were fixed in 100% acetone and air dried. Endogenous peroxidase activity was blocked with peroxidase blocking reagent (Dako). The sections were incubated with purified rat anti–mouse PD-L1 mAb (clone MIH5; eBiosciences). The primary Abs were detected using the Histofine Simple Stain Mouse MAX PO (Rat) kit and DAB solution (Nichirei). The images were captured using an Olympus BH2 microscope with a Nikon DS-5M color digital camera (Nikon), controlled by Nikon ATC-2U software version 1.5. An Olympus ×10/20 ocular lens and a ×20/0.46 NA objective lens were used. Images were cropped using Adobe Photoshop (Adobe Systems) and were composed using Adobe Illustrator.

Statistics. We used the Kaplan-Meier product-limit method to obtain survival probability and the log-rank test to compare survival curves. The Mann-Whitney *U* test was used to analyze the clinical scores. A *P* value less than 0.05 was considered statistically significant.

Acknowledgments

We thank Miyuki Azuma of Tokyo Medical and Dental University for providing hybridoma MIH5-producing anti–PD-L1 mAbs. This study was supported by grant 21390295 from the Ministry of Education, Culture, Sports, Science, and Technology (Tokyo, Japan) (to T. Teshima), Health and Labor Science Research Grants (Tokyo, Japan) (to T. Teshima), and a grant from the Foundation for Promotion of Cancer Research (Tokyo, Japan) (to T. Teshima).

Received for publication March 11, 2009, and accepted in revised form April 7, 2010.

Address correspondence to: Takanori Teshima, Center for Cellular and Molecular Medicine, Kyushu University Hospital, 3-1-1 Maidashi, Higashi-ku, Fukuoka 812-8582, Japan. Phone: 81.92.642.5947; Fax: 81.92.642.5951; E-mail: tteshima@cancer.med.kyushu-u.ac.jp.

1. Weiden P, et al. Antileukemic effect of graft-versus-host disease in human recipients of allogeneic-marrow grafts. *N Engl J Med.* 1979;300(19):1068–1073.
2. Weiden PL, Sullivan KM, Flournoy N, Storb R, Thomas ED. Antileukemic effect of chronic graft-versus-host disease: contribution to improved survival after allogeneic marrow transplantation. *N Engl J Med.* 1981;304(25):1529–1533.
3. Korngold R, Sprent J. Lethal graft-versus-host disease after bone marrow transplantation across minor histocompatibility barriers in mice. Prevention by removing mature T-cells from marrow. *J Exp Med.* 1978;148(6):1687–1698.
4. Apperley JF, Jones L, Hale G, Goldman JM. Bone marrow transplantation for chronic myeloid leukemia: T-cell depletion with Campath-1 reduces the incidence of acute graft-versus-host disease but may increase the risk of leukemia relapse. *Bone Marrow Transplant.* 1986;1(1):53–66.
5. Atkinson K, et al. Risk factors for chronic graft-versus-host disease after HLA-identical sibling bone marrow transplantation. *Blood.* 1990;75(12):2459–2464.
6. Shlomchik WD, et al. Prevention of graft versus host disease by inactivation of host antigen-presenting cells. *Science.* 1999;285(5426):412–415.
7. Reddy P, Maeda Y, Liu C, Krijanovski OI, Korngold R, Ferrara JL. A crucial role for antigen-presenting cells and alloantigen expression in graft-versus-leukemia responses. *Nat Med.* 2005;11(11):1244–1249.
8. Bleakley M, Riddell SR. Molecules and mechanisms of the graft-versus-leukaemia effect. *Nat Rev Cancer.* 2004;4(5):371–380.
9. Teshima T, et al. Acute graft-versus-host disease does not require alloantigen expression on host epithelium. *Nat Med.* 2002;8(6):575–581.
10. Jones SC, Murphy GF, Friedman TM, Korngold R. Importance of minor histocompatibility antigen expression by nonhematopoietic tissues in a CD4+ T cell-mediated graft-versus-host disease model. *J Clin Invest.* 2003;112(12):1880–1886.
11. Ruggeri L, et al. Effectiveness of donor natural killer cell alloreactivity in mismatched hematopoietic transplants. *Science.* 2002;295(5562):2097–2100.
12. Matte CC, et al. Donor APCs are required for maximal GVHD but not for GVL. *Nat Med.* 2004;10(9):987–992.
13. Cooke KR, et al. An experimental model of idiopathic pneumonia syndrome after bone marrow transplantation. I. The roles of minor H antigens and endotoxin. *Blood.* 1996;88(8):3230–3239.
14. Korngold R, Sprent J. Features of T cells causing H-2-restricted lethal graft-vs.-host disease across minor histocompatibility barriers. *J Exp Med.* 1982;155(3):872–883.
15. Zhang Y, Joe G, Hexner E, Zhu J, Emerson SG. Alloreactive memory T cells are responsible for the persistence of graft-versus-host disease. *J Immunol.* 2005;174(5):3051–3058.
16. Stefanova I, Dorfman JR, Germain RN. Self-recognition promotes the foreign antigen sensitivity of naive T lymphocytes. *Nature.* 2002;420(6914):429–434.
17. Zhang Y, Louboutin JP, Zhu J, Rivera AJ, Emerson SG. Preterminal host dendritic cells in irradiated mice prime CD8+ T cell-mediated acute graft-versus-host disease. *J Clin Invest.* 2002;109(10):1335–1344.
18. Zajac AJ, et al. Viral immune evasion due to persistence of activated T cells without effector function. *J Exp Med.* 1998;188(12):2205–2213.
19. Barber DL, et al. Restoring function in exhausted CD8 T cells during chronic viral infection. *Nature.* 2006;439(7077):682–687.
20. Shin H, Wherry EJ. CD8 T cell dysfunction during chronic viral infection. *Curr Opin Immunol.* 2007;19(4):408–415.
21. Keir ME, Butte MJ, Freeman GJ, Sharpe AH. PD-1 and its ligands in tolerance and immunity. *Annu Rev Immunol.* 2008;26:677–704.
22. Dong H, et al. Tumor-associated B7-H1 promotes T-cell apoptosis: a potential mechanism of immune evasion. *Nat Med.* 2002;8(8):793–800.
23. Ahmadzadeh M, et al. Tumor antigen-specific CD8

T cells infiltrating the tumor express high levels of PD-1 and are functionally impaired. *Blood.* 2009; 114(8):1537–1544.
24. Zhang L, Gajewski TF, Kline J. PD-1/PD-L1 interactions inhibit anti-tumor immune responses in a murine acute myeloid leukemia model. *Blood.* 2009; 114(8):1545–1552.
25. Mumprecht S, Schurch C, Schwaller J, Solenthaler M, Ochsenbein AF. PD-1 signaling on chronic myeloid leukemia-specific T cells results in T cell exhaustion and disease progression. *Blood.* 2009; 114(8):1528–1536.
26. Iwai Y, Terawaki S, Ikegawa M, Okazaki T, Honjo T. PD-1 inhibits antiviral immunity at the effector phase in the liver. *J Exp Med.* 2003;198(1):39–50.
27. Horowitz MM, et al. Graft-versus-leukemia reactions after bone marrow transplantation. *Blood.* 1990;75(3):555–562.
28. Gallimore A, et al. Induction and exhaustion of lymphocytic choriomeningitis virus-specific cytotoxic T lymphocytes visualized using soluble tetrameric major histocompatibility complex class I-peptide complexes. *J Exp Med.* 1998;187(9):1383–1393.
29. Welsh RM. Assessing CD8 T cell number and dysfunction in the presence of antigen. *J Exp Med.* 2001; 193(5):F19–F22.
30. Moskophidis D, Lechner F, Pircher H, Zinkernagel RM. Virus persistence in acutely infected immunocompetent mice by exhaustion of antiviral cytotoxic effector T cells. *Nature.* 1993;362(6422):758–761.
31. Appay V, et al. HIV-specific CD8(+) T cells produce antiviral cytokines but are impaired in cytolytic function. *J Exp Med.* 2000;192(1):63–75.
32. Xiong Y, et al. Simian immunodeficiency virus (SIV) infection of a rhesus macaque induces SIV-specific CD8(+) T cells with a defect in effector function that is reversible on extended interleukin-2 incubation. *J Virol.* 2001;75(6):3028–3033.
33. Pantaleo G, Harari A. Functional signatures in antiviral T-cell immunity for monitoring virus-associated diseases. *Nat Rev Immunol.* 2006;6(5):417–423.
34. Tham EL, Mescher MF. Signaling alterations in activation-induced nonresponsive CD8 T cells. *J Immunol.* 2001;167(4):2040–2048.
35. Tham EL, Shrikant P, Mescher MF. Activation-induced nonresponsiveness: a Th-dependent regulatory checkpoint in the CTL response. *J Immunol.* 2002;168(3):1190–1197.
36. Boissonnas A, et al. Antigen distribution drives programmed antitumor CD8 cell migration and determines its efficiency. *J Immunol.* 2004;173(1):222–229.
37. Saito T, Dworacki G, Gooding W, Lotze MT, Whiteside TL. Spontaneous apoptosis of CD8+ T lymphocytes in peripheral blood of patients with advanced melanoma. *Clin Cancer Res.* 2000;6(4):1351–1364.
38. Fontaine P, Roy-Proulx G, Knafo L, Baron C, Roy DC, Perreault C. Adoptive transfer of minor histocompatibility antigen-specific T lymphocytes eradicates leukemia cells without causing graft-versus-host disease. *Nat Med.* 2001;7(7):789–794.
39. Meunier MC, Roy-Proulx G, Labrecque N, Perreault C. Tissue distribution of target antigen has a decisive influence on the outcome of adoptive cancer immunotherapy. *Blood.* 2003;101(2):766–770.
40. Dickinson AM, et al. In situ dissection of the graft-versus-host activities of cytotoxic T cells specific for minor histocompatibility antigens. *Nat Med.* 2002; 8(4):410–414.
41. Ding ZC, Blazar BR, Mellor AL, Munn DH, Zhou G. Chemotherapy rescues tumor-driven aberrant CD4+ T-cell differentiation and restores an activated polyfunctional helper phenotype. *Blood.* 2010; 115(12):2397–2406.
42. Tanaka K, et al. PDL1 is required for peripheral transplantation tolerance and protection from chronic allograft rejection. *J Immunol.* 2007; 179(8):5204–5210.
43. Haspot F, et al. Peripheral deletional tolerance of alloreactive CD8 but not CD4 T cells is dependent on the PD-1/PD-L1 pathway. *Blood.* 2008; 112(5):2149–2155.
44. Yamazaki T, et al. Expression of programmed death 1 ligands by murine T cells and APC. *J Immunol.* 2002;169(10):5538–5545.
45. Keir ME, et al. Tissue expression of PD-L1 mediates peripheral T cell tolerance. *J Exp Med.* 2006; 203(4):883–895.
46. Crawford A, Wherry EJ. The diversity of costimulatory and inhibitory receptor pathways and the regulation of antiviral T cell responses. *Curr Opin Immunol.* 2009;21(2):179–186.
47. Blackburn SD, et al. Coregulation of CD8+ T cell exhaustion by multiple inhibitory receptors during chronic viral infection. *Nat Immunol.* 2009; 10(1):29–37.
48. Petrovas C, et al. PD-1 is a regulator of virus-specific CD8+ T cell survival in HIV infection. *J Exp Med.* 2006;203(10):2281–2292.
49. Brooks DG, Trifilo MJ, Edelmann KH, Teyton L, McGavern DB, Oldstone MB. Interleukin-10 determines viral clearance or persistence in vivo. *Nat Med.* 2006;12(11):1301–1309.
50. Blackburn SD, Shin H, Freeman GJ, Wherry EJ. Selective expansion of a subset of exhausted CD8 T cells by alphaPD-L1 blockade. *Proc Natl Acad Sci U S A.* 2008;105(39):15016–15021.
51. Kaufmann DE, et al. Upregulation of CTLA-4 by HIV-specific CD4+ T cells correlates with disease progression and defines a reversible immune dysfunction. *Nat Immunol.* 2007;8(11):1246–1254.
52. Franceschini D, et al. PD-L1 negatively regulates CD4+CD25+Foxp3+ Tregs by limiting STAT-5 phosphorylation in patients chronically infected with HCV. *J Clin Invest.* 2009;119(3):551–564.
53. Socie G, Blazar BR. Acute graft-versus-host disease: from the bench to the bedside. *Blood.* 2009; 114(20):4327–4336.
54. Blazar BR, et al. Blockade of programmed death-1 engagement accelerates graft-versus-host disease lethality by an IFN-gamma-dependent mechanism. *J Immunol.* 2003;171(3):1272–1277.
55. Brochu S, Rioux-Masse B, Roy J, Roy DC, Perreault C. Massive activation-induced cell death of alloreactive T cells with apoptosis of bystander postthymic T cells prevents immune reconstitution in mice with graft-versus-host disease. *Blood.* 1999;94(2):390–400.
56. Dey B, et al. The fate of donor T-cell receptor transgenic T cells with known host antigen specificity in a graft-versus-host disease model. *Transplantation.* 1999;68(1):141–149.
57. Choi EY, et al. Real-time T-cell profiling identifies H60 as a major minor histocompatibility antigen in murine graft-versus-host disease. *Blood.* 2002; 100(13):4259–4265.
58. Michalek J, Collins RH, Hill BJ, Brenchley JM, Douek DC. Identification and monitoring of graft-versus-host specific T-cell clone in stem cell transplantation. *Lancet.* 2003;361(9364):1183–1185.
59. Hirano F, et al. Blockade of B7-H1 and PD-1 by monoclonal antibodies potentiates cancer therapeutic immunity. *Cancer Res.* 2005;65(3):1089–1096.
60. Ando K, et al. Perforin, Fas/Fas ligand, and TNF-alpha pathways as specific and bystander killing mechanisms of hepatitis C virus-specific human CTL. *J Immunol.* 1997;158(11):5283–5291.
61. Tsushima F, et al. Preferential contribution of B7-H1 to programmed death-1-mediated regulation of hapten-specific allergic inflammatory responses. *Eur J Immunol.* 2003;33(10):2773–2782.
62. Teshima T, et al. IL-11 separates graft-versus-leukemia effects from graft-versus-host disease after bone marrow transplantation. *J Clin Invest.* 1999;104(3):317–325.

blood

2010 116: 5119-5125
Prepublished online September 7, 2010;
doi:10.1182/blood-2010-06-289231

Hepatic toxicity and prognosis in hepatitis C virus–infected patients with diffuse large B-cell lymphoma treated with rituximab-containing chemotherapy regimens: a Japanese multicenter analysis

Daisuke Ennishi, Yoshinobu Maeda, Nozomi Niitsu, Minoru Kojima, Koji Izutsu, Jun Takizawa, Shigeru Kusumoto, Masataka Okamoto, Masahiro Yokoyama, Yasushi Takamatsu, Kazutaka Sunami, Akira Miyata, Kayoko Murayama, Akira Sakai, Morio Matsumoto, Katsuji Shinagawa, Akinobu Takaki, Keitaro Matsuo, Tomohiro Kinoshita and Mitsune Tanimoto

Blood (print ISSN 0006-4971, online ISSN 1528-0020), is published weekly by the American Society of Hematology, 2021 L St, NW, Suite 900, Washington DC 20036.

Hepatic toxicity and prognosis in hepatitis C virus–infected patients with diffuse large B-cell lymphoma treated with rituximab-containing chemotherapy regimens: a Japanese multicenter analysis

Daisuke Ennishi,[1] Yoshinobu Maeda,[1] Nozomi Niitsu,[2] Minoru Kojima,[3] Koji Izutsu,[4] Jun Takizawa,[5] Shigeru Kusumoto,[6] Masataka Okamoto,[7] Masahiro Yokoyama,[8] Yasushi Takamatsu,[9] Kazutaka Sunami,[10] Akira Miyata,[11] Kayoko Murayama,[12] Akira Sakai,[13] Morio Matsumoto,[14] Katsuji Shinagawa,[1] Akinobu Takaki,[15] Keitaro Matsuo,[16] Tomohiro Kinoshita,[17] and Mitsune Tanimoto[1]

[1]Department of Hematology, Oncology and Respiratory Medicine, Okayama University Graduate School of Medicine, Dentistry and Pharmaceutical Sciences, Okayama; [2]Department of Hematology, Saitama Medical University International Medical Center, Hidaka; [3]Department of Hematology and Oncology, Tokai University, Isehara; [4]Division of Hematology, Kanto Medical Center NTT EC, Tokyo; [5]Division of Hematology, Niigata University Graduate School of Medical & Dental Sciences, Niigata; [6]Department of Medical Oncology and Immunology, Nagoya City University Graduate School of Medical Sciences, Nagoya; [7]Department of Hematology and Oncology, Fujita-Health University School of Medicine, Toyoake; [8]Medical Oncology/Hematology, Cancer Institute Hospital, Tokyo; [9]Department of Oncology Hematology, Fukuoka University Hospital, Fukuoka; [10]Internal Medicine, National Okayama Medical Center, Okayama; [11]Department of Hematology, Chugoku Chuo Hospital, Fukuyama; [12]Department of Hematology, Gunma Prefectural Cancer Canter, Ota; [13]Department of Hematology, Hiroshima University, Hiroshima; [14]Department of Hematology, Nishigunma National Hospital, Shibukawa; [15]Department of Gastroenterology and Hepatology, Okayama University Graduate School of Medicine, Dentistry and Pharmaceutical Sciences, Okayama; [16]Division of Epidemiology and Prevention, Aichi Cancer Center Institute, Nagoya; and [17]Department of Hematology and Oncology, Nagoya University Graduate School of Medicine, Nagoya, Japan

The influence of hepatitis C virus (HCV) infection on prognosis and hepatic toxicity in patients with diffuse large B-cell lymphoma in the rituximab era is unclear. Thus, we analyzed 553 patients, 131 of whom were HCV-positive and 422 of whom were HCV-negative, with DLBCL treated with rituximab, cyclophosphamide, doxorubicin, vincristine, and prednisone (RCHOP)–like chemotherapy. Survival outcomes and hepatic toxicity were compared according to HCV infection. The median follow-up was 31 and 32 months for patients who were HCV-positive and HCV-negative, respectively. HCV infection was not a significant risk factor for prognosis (3-year progression-free survival, 69% vs 77%, $P = .22$; overall survival, 75% vs 84%, $P = .07$). Of 131 patients who were HCV-positive, 36 (27%) had severe hepatic toxicity (grade 3-4), compared with 13 of 422 (3%) patients who were HCV-negative. Multivariate analysis revealed that HCV infection was a significant risk factor for severe hepatic toxicity (hazard ratio: 14.72; 95% confidence interval, 6.37-34.03; $P < .001$). An exploratory analysis revealed that pretreatment transaminase was predictive of severe hepatic toxicity. HCV-RNA levels significantly increased during immunochemotherapy ($P = .006$). These results suggest that careful monitoring of hepatic function and viral load is indicated during immunochemotherapy for HCV-positive patients. (*Blood*. 2010; 116(24):5119-5125)

Introduction

Many epidemiologic studies have demonstrated an association between hepatitis C virus (HCV) infection and non-Hodgkin lymphoma, suggesting that HCV plays a role in the development of this malignancy.[1-8] Fewer data are available for patients who are HCV-positive with diffuse large B-cell lymphoma (DLBCL), as low-grade marginal zone lymphoma is the most common lymphoma subtype associated with HCV infection.[3,8] Thus, studies comparing DLBCL outcomes based on HCV infection are extremely rare, and the prognostic value of HCV infection remains controversial, because of heterogeneity in histology and treatment strategies.[9,10] Several series have shown good tolerance to standard chemotherapy for lymphoma patients who are infected with HCV.[9-11] However, these studies were conducted in the pre-rituximab era.

Although the cyclophosphamide, doxorubicin, vincristine, and prednisone (CHOP) regimen has been the mainstay treatment for aggressive lymphomas for several decades,[12] treatment outcomes have improved significantly since the introduction of rituximab (an anti-CD20 chimeric antibody) in both young and elderly patients.[13-15] Since the introduction of rituximab, several prognostic factors have been reevaluated in DLBCL patients,[16-18] but the prognostic value of HCV infection in rituximab combination chemotherapy has not been well established. In addition, hepatitis B virus (HBV) reactivation is a well-documented complication that occurs frequently after introduction of rituximab.[19,20] However, no large-scale study has investigated the influence of HCV infection on hepatic toxicity in patients with DLBCL treated with rituximab-containing chemotherapy.

Submitted June 25, 2010; accepted August 21, 2010. Prepublished online as *Blood* First Edition paper, September 7, 2010; DOI 10.1182/blood-2010-06-289231.

An Inside *Blood* analysis of this article appears at the front of this issue.

The online version of this article contains a data supplement.

This study was presented in part at the 51st annual meeting of the American Society of Hematology, New Orleans, LA, December 5-8, 2009.

The publication costs of this article were defrayed in part by page charge payment. Therefore, and solely to indicate this fact, this article is hereby marked "advertisement" in accordance with 18 USC section 1734.

We conducted a multicenter retrospective analysis to compare the prognosis and hepatic toxicity of untreated patients with DLBCL uniformly receiving rituximab plus CHOP-like chemotherapy according to HCV infection.

Methods

Patients

We collected medical information from patients who were HCV-positive with DLBCL, who received rituximab plus CHOP (RCHOP)-like therapy as a first-line treatment at 32 participating Japanese institutions between January 2004 and April 2008, and who were followed until March 2009. We also collected medical information from patients who were HCV-negative, treated within 2 months of the treatment start date for each patient who was HCV-positive. This study protocol was approved by the institutional review boards of each participating institute and complied with all provisions of the Declaration of Helsinki. DLBCL was diagnosed by an expert hematopathologist at each institute, based on the World Health Organization classification.[21] Patients were included if they were more than 20 years old, and an HCV infection test was performed before treatment. Both de novo DLBCL and transformed DLBCL (t-DLBCL) from low-grade B-cell lymphomas were included. Patients were excluded if they were positive for hepatitis B surface antigen (HBsAg) or for human immunodeficiency virus-1 or -2 antigens. Patients with primary central nervous system lymphoma, primary testicular lymphoma, and intravascular large-cell lymphoma (IVL) were also excluded.

In total, 590 patients, including 136 with and 454 without HCV infection, were registered. Then, 37 patients were excluded for the following reasons: HBsAg-positive (n = 2), non–rituximab-containing regimen (n = 2), absence of final outcome data (n = 1) in patients who were HCV-positive; except the definitive period corresponding to each patient who was HCV-positive (n = 26), regimens other than RCHOP-like (n = 3), HBsAg-positive (n = 2), and IVL (n = 1) in patients who were HCV-negative. In total, 553 patients were eligible; 131 patients (23.7%) were HCV-positive, whereas 422 (76.3%) were HCV-negative.

Clinical and laboratory information, including antibodies to HBsAg (anti-HBs) and hepatitis B core antigen (anti-HBc), was available at the time of diagnosis. HCV infection was defined as the detection of anti-HCV antibodies with commercially available second- or third-generation immunoassay kits (Monolisa anti-HCV Plus, Sanofi Diagnostics Pasteur; and Axsym HCV Version 3.0, Abbott Laboratories).

Treatment and response assessment

All DLBCL patients with HCV infection during the definitive period received immunochemotherapy. Chemotherapy regimens included RCHOP, rituximab plus cyclophosphamide, therarubicin, vincristine, and prednisone, and rituximab plus cyclophosphamide, epirubicin, vincristine, and prednisone. Disease stage was evaluated using the Ann Arbor staging system. Liver and spleen involvement was diagnosed by imaging lymphoma invasion, such as nodular lesions or heterogeneous concentrations. Chemotherapy sensitivity was defined according to standard volume criteria, using computed tomography (CT) and positron emission tomography (PET)/CT with [^{18}F]-fluorodeoxyglucose imaging.[22,23]

Liver function tests and HCV viral markers

In all patients enrolled, pretreatment levels of alanine aminotransferase (ALT) and aspartate aminotransferase (AST) and their highest levels up to 6 months after completing immunochemotherapy were collected for analysis. Hepatic toxicity was defined by the National Cancer Institute of Canada criteria, and severe hepatic toxicity was defined as an increase in transaminase levels (AST or ALT, grade 3 or 4; $> 5.0 \times$ ULN). To assess impaired hepatic synthesis, serum total bilirubin (T-Bil), albumin (Alb), prothrombin time, and platelet counts were collected at the time of DLBCL diagnosis and at 1 and 6 months after treatment. Serum HCV RNA load was determined by quantitative reverse-transcription polymerase chain reaction (detection value of 5-5000 KIU/mL; Amplicor HCV Monitor Test, Version 2.0, Cobas-High-Range assay, Roche Diagnostics).

Statistical analyses

Progression-free survival (PFS) was calculated from the treatment initiation date to the date of documented disease progression, relapse, or the end date of the study. Non–lymphoma-related deaths were censored for PFS. Overall survival (OS) was calculated from the treatment initiation date until death from any cause or the last follow-up. If the stop date was not reached, the data were censored at the date of the last follow-up evaluation. Survival curves were created by the Kaplan-Meier method, and overall differences were compared using the log-rank test. Multivariate analysis was performed using a Cox proportional hazard model to estimate the independent impact of HCV infection on survival and severe hepatic toxicity. In patients who were HCV-positive, risk factors for severe hepatic toxicity were also evaluated by multivariate analysis. Changes in transaminase levels with respect to HCV infection were compared using the Kruskal-Wallis test. Intraindividual changes in serum HCV-RNA levels were assessed using the Wilcoxon signed-rank test. We evaluated impaired hepatic synthesis according to HCV infection using a univariate linear regression model. The basic characteristics and outcomes of each group (HCV-positive and -negative) were compared using the χ^2 test, t test, and the Mann-Whitney U test, as appropriate. All statistical tests were 2-sided, and the differences were deemed to be statistically significant if $P < .05$. Data were analyzed using the Stata software Version 10 (StataCorp LP).

Results

Patient characteristics

Patient characteristics are listed in Table 1. The median age of all patients was 68 years (range, 20-92 years). Before treatment, patients who were HCV-positive were older ($P < .001$), had more frequently elevated lactate dehydrogenase levels ($P = .002$), more than 2 extranodal sites ($P = .02$), spleen involvement ($P = .001$), and a higher international prognostic index (IPI) ($P = .01$) than patients who were HCV-negative. There was no difference in the occurrence of t-DLBCL according to HCV infection.

Of the patients who were HCV-positive at the time of DLBCL diagnosis, 57 (43%) and 20 (15%) patients were known to have chronic hepatitis (CH) and liver cirrhosis (LC), respectively. Hepatocellular carcinoma (HCC) complications were detected in 7 patients (5%) before immunochemotherapy. The diagnosis of HCC was made by CT or magnetic resonance imaging in 3 patients and by biopsy in 4 patients. Seven patients with CH and one patient with LC were HB serology-positive. One HB serology-positive patient was given prophylactic lamivudine treatment during immunochemotherapy. Twelve patients (9%) had a history of anti-HCV therapy before DLBCL treatment, 2 patients continued anti-HCV therapy during immunochemotherapy, and 5 patients restarted anti-HCV therapy after immunochemotherapy.

Survival analysis

The median follow-up time was 31 months (range, 4-42 months) for patients who were HCV-positive and 32 months (range, 5-51 months) for those who were HCV-negative. Complete remission (CR) or uncertain CR rates were 81% and 83% in HCV-positive and HCV-negative patients, respectively. No significant difference was observed in PFS according to HCV infection (3-year PFS, 69% vs 77%, $P = .22$). The OS tended to be worse in patients who were HCV-positive than in those who were HCV-negative (3-year OS, 75% vs 84%, $P = .07$; Figure 1A-B). The PFS and OS rates at 3 years were 56% and 64% for high IPI or

Table 1. Comparison of HCV-positive with HCV-negative patients

	HCV-positive (n = 131), n (%)	HCV-negative (n = 422), n (%)	*P*
Median age, y (range)	70.4 (42-86)	64.3 (20-92)	< .001
Sex, male/female	79/52	228/194	.21
LDH > normal	81 (62)	196 (46)	.002
PS > 1	16 (12)	40 (9)	.47
Stage			.48
I	28 (21)	92 (22)	
II	39 (30)	130 (31)	
III	20 (15)	84 (20)	
IV	44 (34)	116 (27)	
Extranodal sites > 1	36 (27)	75 (18)	.02
IPI: H/I, H	53 (40)	139 (33)	.01
BM involvement	12 (9)	38 (9)	.96
Spleen involvement	24 (18)	35 (8)	.001
Liver involvement	12 (9)	25 (6)	.20
t-DLBCL	5 (4)	11 (3)	.82
FL	3	5	
MZBCL	2	6	
HBsAb-positive	7/59 (12)	13/135 (10)	.24
HBcAb-positive	11/22 (50)	9/57 (16)	.03
Treatment			.12
RCHOP	96 (73)	339 (80)	
RTHPCOP	31 (24)	71 (17)	
RCEOP	4 (3)	12 (3)	
Baseline transaminase			.48
Grade 0-1	122 (93)	415 (98)	
Grade 2	7 (5)	3 (1)	
Grade 3	2 (2)	4 (1)	
Outcome of patients			
Died of lymphoma	14 (11)	45 (11)	.87
Died of hepatic failure	6 (5)	1 (0.2)	< .001
Died of other causes	4 (3)	7 (2)	.76
Hepatic toxicity			
Grade 3-4	36 (27)	13 (3)	< .001

LDH indicates lactate dehydrogenase; PS, ECOG performance status; H/I, high-intermediate; H, high; BM, bone marrow; t-DLBCL, transformed diffuse large B-cell lymphoma; FL, follicular lymphoma; MZBCL, marginal zone B-cell lymphoma; HBsAb, antibody to hepatitis B surface antigen; HBcAb, antibody to hepatitis B core antigen; RCHOP, rituximab plus cyclophosphamide, doxorubicin, vincristine, and prednisone; RTHPCOP, rituximab plus cyclophosphamide, teralbicin, vincristine, and prednisone; and RCEOP, rituximab plus cyclophosphamide, epirubicin, vincristine, and prednisone. Grade was defined by the National Cancer Institute of Canada criteria.

high-intermediate and 81% and 88% for low IPI or low-intermediate, respectively. In these cases there were significant differences in the PFS and OS rates (both $P < .001$). Cox multivariate analysis showed that older age and advanced stage had significant adverse effects on OS. In contrast, HCV infection was not associated with poor PFS or OS (Table 2). According to the cause-specific analysis, survival rates for lymphoma did not significantly correlate with HCV infection (3-year, 84% vs 86%; $P = .80$).

Hepatic toxicity

The pretreatment transaminase levels were not significantly different in patients with HCV infection (Table 1). Of the 131 patients who were HCV-positive, 36 (27%) had severe hepatic toxicity, compared with 3% of those who were HCV-negative. Multivariate analysis revealed that HCV infection was a significant risk factor for severe hepatic toxicity (hazard ratio [HR]: 14.72; 95% confidence interval [CI], 6.37-34.03; $P < .001$; supplemental Table 1, available on the *Blood* Web site; see the Supplemental Materials link at the top of the online article). The changes in AST and ALT levels with respect to HCV infection were significant (both $P < .001$; Figure 2A-B). The median time from treatment initiation to the development of severe hepatic toxicity was 103 days

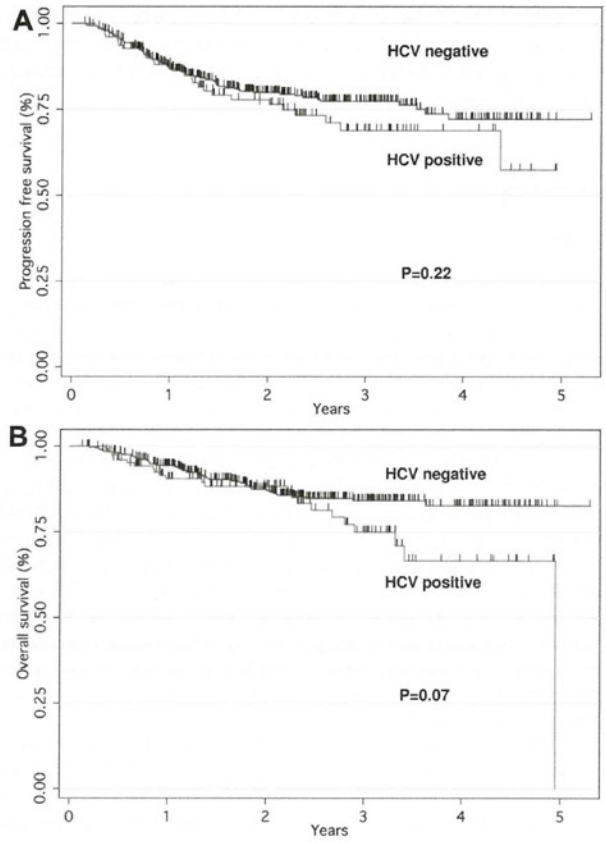

Figure 1. PFS and OS curves for patients with DLBCL treated with RCHOP according to HCV infection. PFS (A) and OS (B) curves based on patients who were HCV-positive (n = 131) versus HCV-negative (n = 422).

Table 2. Multivariate analysis of survival

	PFS			OS		
Characteristic	**HR**	**95% CI**	***P***	**HR**	**95% CI**	***P***
HCV infection						
Negative	1.00	Ref		1.00	Ref	
Positive	0.97	0.59-1.60	NS	1.22	0.69-2.15	NS
Sex						
Male	1.00	Ref		1.00	Ref	
Female	1.47	0.98-2.22	NS	1.44	0.88-2.37	NS
Age, y						
20-60	1.00	Ref		1.00	Ref	
> 60	1.02	1.01-1.04	.01	1.03	1.01-1.06	.007
LDH						
Normal	1.00	Ref		1.00	Ref	
> Normal	1.16	0.72-1.87	NS	1.37	0.77-2.43	NS
PS						
0-1	1.00	Ref		1.00	Ref	
2-4	1.28	1.04-1.59	.02	1.16	0.89-1.51	NS
Extranodal sites						
0 or 1	1.00	Ref		1.00	Ref	
2	0.77	0.45-1.30	NS	0.87	0.45-1.68	NS
Stage						
I, II	1.00	Ref		1.00	Ref	
III, IV	1.64	1.28-2.11	< .001	1.67	1.20-2.32	.002

Ref indicates reference; and NS, not significant.

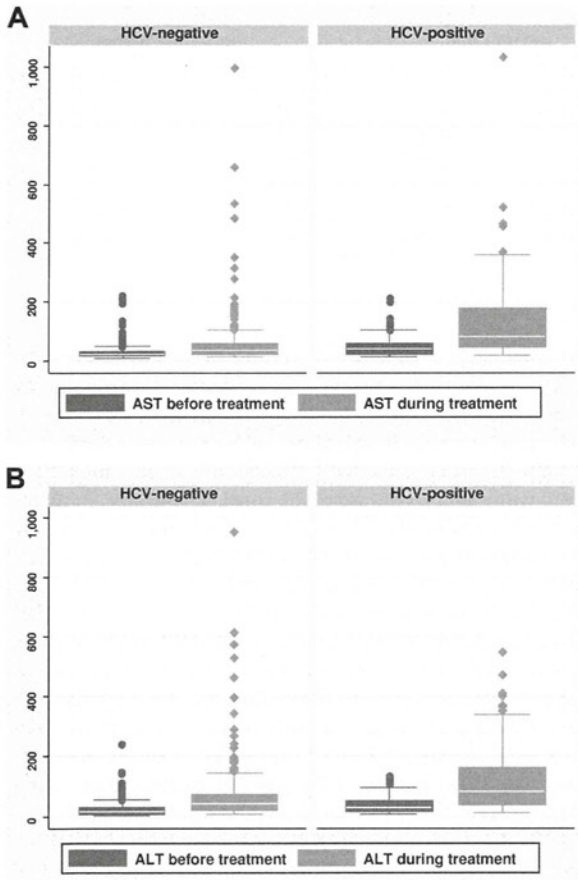

Figure 2. The changes of AST and ALT levels between before treatment levels and highest levels up to 6 months after completing immunochemotherapy. The changes in AST (A) and ALT (B) levels with respect to HCV infection were significant (both $P < .001$).

(range, 8-320 days). In those who were HCV-positive, pretreatment transaminase levels were significant risk factors (HR, 6.42; 95% CI, 1.11-37.12; $P < .001$) for severe hepatic toxicity among baseline characteristics (supplemental Table 2). In HCV-positive patients, severe hepatic toxicity was observed in 6 (33%) of 18 patients and 30 (27%) of 113 patients with and without omission of prednisone, respectively ($P = .82$).

Severe hepatic toxicity was not associated with poor PFS or OS in patients who were HCV-positive ($P = .56$ and $P = .51$, respectively). However modification of the scheduled dose was required for 16 patients because of severe hepatic toxicity, and chemotherapy was withdrawn for 6 patients, including 2 who died because of disease progression (Table 3). The remaining 4 patients stopped immunochemotherapy; however, they received radiation therapy after their liver function normalized or they discontinued treatment, and they were alive and in remission.

Changes in serum T-Bil, Alb, platelet counts, and prothrombin time showed no difference with regard to HCV infection status (supplemental Figure 1). Progression of hepatic complications during treatment occurred in 4 cases; progression from CH to LC, and from LC to HCC, occurred in 2 patients each.

Of the 24 deaths in patients who were HCV-positive, 14 were caused by disease progression, and 6 were caused by hepatic failure (Table 4). The 4 remaining deaths were caused by 2 cardiovascular and 2 brain vascular events. Among HCV-positive patients, HCC was predictive of death from hepatic failure (supplemental Table 3).

In total, 36 HCV-positive patients developed severe hepatic toxicity. At the time they developed severe hepatic toxicity, 29 patients were negative for either HBsAg or HBV-DNA, and 7 patients had no data about HBsAg or HBV-DNA. None of the 36 patients received any anti-HBV viral therapy, such as lamivudine.

HCV viral load

HCV-RNA levels were collected during pretreatment (n = 79), at the highest levels during the period of treatment initiation to 1 mo after treatment completion (n = 47), and 1-6 months after treatment (n = 44). HCV-RNA levels for all 3 time points were available from 34 patients. Mean HCV-RNA levels at the 3 time points as determined from those samples were 1001 (95% CI, 522-1481), 3187 (2148-4232), and 1986 (1145-2827) KIU/mL, indicating that HCV-RNA increased significantly during immunochemotherapy ($P = .006$) but then decreased afterward ($P = .003$; Figure 3). In 2 patients who received antiviral therapy during immunochemotherapy, HCV-RNA levels increased after the initiation of immunochemotherapy. In 3 cases where HCV-RNA was under the threshold level (< 5 KIU/mL) before treatment, HCV-RNA increased, more than 100-fold, and 2 patients developed severe hepatic toxicity (Table 5).

Discussion

This study showed that prognosis did not differ according to HCV infection. In sharp contrast, the incidence of severe hepatic toxicity was high in HCV-positive patients, and HCV infection was determined to be a strong risk factor for this adverse effect. These findings were not consistent with previous reports demonstrating good tolerance for HCV infection in the pre-rituximab era.[8,10,11,24] This is the first large study to show the influence of HCV infection on prognosis and hepatic toxicity in patients with DLBCL in the rituximab era.

A previous report showed that HCV-positive patients with DLBCL exhibited worse OS, but not event-free survival; however, this study included a very small number of HCV-positive patients

Table 3. Details and outcomes of 6 patients withdrawn from immunochemotherapy due to severe hepatic toxicity

Case	Age, y	Sex	Stage	Hepatic disease at baseline	AST/ALT at baseline, IU/L	AST/ALT peak level, IU/L	No. of cycles of treatment before withdrawal	Outcome
1	76	F	III	LC	101/73	236/114	4	Died of lymphoma progression
2	78	F	III	CH	38/25	1033/340	1	Died of lymphoma progression
3	71	F	I	LC	90/82	289/128	1	Alive
4	59	M	IV	CH	31/17	211/284	4	Alive
5	74	F	IV	Normal	50/29	274/302	3	Alive
6	76	M	II	Normal	19/25	522/550	3	Alive

Table 4. Details of 6 patients who died due to hepatic failure

Case	Age, y	Sex	Stage	Treatment	Hepatic disease at baseline	AST/ALT, IU/L		HCV-RNA, KIU/mL	
						At baseline	Peak level	At baseline	Peak level during treatment
1	75	M	I	RCEOP	LC	91/63	136/102	ND	1000
2	74	F	IV	RTHPCOP	HCC	29/16	58/49	4400	5000
3	68	F	II	RTHPCOP	CH	118/76	203/113	510	1600
4	71	F	III	RCHOP	HCC	34/41	242/139	470	ND
5	64	M	IV	RCHOP	HCC	27/10	97/32	ND	ND
6	76	M	III	RTHPCOP	HCC	46/40	111/107	434	21 300

ND indicates not done.

(n = 23) and was based on short-term follow-up.[9] Another large scale study of DLBCL demonstrated that the 5-year PFS was 51% and OS was 72%, but the relationship between HCV infection and outcome in this study remained unclear, because of the lack of an HCV-negative control group.[10] In addition, these studies were performed in the pre-rituximab era, and no large-scale study has compared the outcome for DLBCL treated with rituximab according to HCV infection. The present study found that HCV-positive patients exhibited more aggressive baseline behavior, consistent with previous reports. These patients also exhibited borderline poor OS by univariate analysis. However, it is important to note that no significant difference was observed in CR rates or PFS according to HCV infection, and multivariate analysis revealed that HCV infection was not a significant risk factor for prognosis.

In the pre-rituximab era, several series showed good tolerance to standard chemotherapy for HCV-infected patients with lymphoma or other hematologic malignancies, with greater than grade 3 liver dysfunction in 10%-18% of patients, and grades 1-4 liver dysfunction in 24% of patients.[10,11,25] In contrast, Besson et al found a higher incidence of toxic deaths among HCV-positive DLBCL patients compared with HCV-negative patients, although this study was based on patients treated with more aggressive chemotherapy than the standard CHOP regimen.[9] A recent analysis also showed an increase in hepatic toxicity in HCV-positive patients with B-cell lymphoma.[26] However, this study included no control group of HCV-negative patients and included heterogeneous treatment strategies and several lymphoma subtypes. In addition, previous series did not exclude HBsAg-positive patients, known to be a high-risk population for severe hepatic injury or fulminant hepatitis.[9-11,25,26] Our study showed that the incidence in severe hepatic toxicity in HCV-positive patients was significantly higher than that of HCV-negative patients (27% vs 3%; $P < .001$), and that these hepatic toxicities led to modification and discontinuation of immunochemotherapy, resulting in lymphoma progression. Careful monitoring of hepatic function should, thus, be recommended for HCV-positive patients, particularly those with high levels of pretreatment transaminase.

Recent case reports have suggested that combined use of rituximab and chemotherapy poses an additional risk for exacerbation of HCV infection.[27-29] However, HCV replication during chemotherapy has not been well characterized. In the present study, monitoring of HCV viral load demonstrated a marked enhancement in HCV replication, and it is suggested that increased HCV expansion results in severe hepatic toxicity. Thus, HCV viral load should also be carefully monitored in HCV-positive patients who receive immunochemotherapy, although this finding must be considered with caution because of the small sample size. In addition, this study revealed that HCV-RNA levels could increase during immunochemotherapy, even though HCV-RNA levels were extremely low (< 5 KIU/mL) before treatment.

Recent reports have indicated that HBsAg-negative/anti-HBc or HBs-positive patients could also develop HBV reactivation after rituximab treatment.[30,31] Among the HCV-positive patients analyzed in the present study for HBV-DNA and HBsAg at the time of hepatic dysfunction, none was positive, and in all patients, severe hepatic toxicity improved with no anti-HBV treatment. In addition, neither anti-HBs– nor anti-HBc–positive patients were found to be in a significant risk group for severe hepatitis (anti-HBs; HR, 0.42; 95% CI, 0.03-5.81, anti-HBc; HR, 0.23; 95% CI, 0.01-1.98). Although we could not completely rule out the possibility of HBV reactivation, we suggest that HCV rather than HBV contributed to severe hepatic toxicity in the present cohort infected with HCV.

In accordance with previous reports,[9-11] HCV-positive patients in the present unmatched study had more aggressive tumor behavior at baseline and more frequent spleen involvement. The mechanisms underlying the association of HCV infection with aggressive tumor behavior are not well understood. Further studies of the biological features of HCV-infected DLBCL, such as germinal center phenotype, are necessary.

HCV infection results in a long-term risk for progression to LC and HCC. One study reported a rapid progression of hepatitis C in patients with humoral immunodeficiency disorders,[32] and an increased rate for liver fibrosis progression was observed in HCV-infected patients who received an allogeneic bone marrow transplant.[33] A possible explanation for the genesis of cirrhosis could be an immune imbalance or impaired regulation of B and T cells.[32,33] We showed that hepatic synthesis after treatment was not affected by HCV infection. However, hepatic disease progressed in 4 patients, and HCC was found to significantly increase the risk of death of hepatic failure, even during short-term observation. Further studies are necessary to clarify the contribution of rituximab to the risk of progressive liver damage.

Table 5. Details and outcomes of the 3 DLBCL patients with HCV-RNA below threshold level before immunochemotherapy

Case	Age, y	Sex	HCV-RNA level, KIU/mL			AST/ALT, IU/L			Outcome/follow-up time, (mo)
			At baseline	Peak level during treatment	At last evaluation	At baseline	Peak level during treatment	At last evaluation	
1	59	M	< 5	3960	79	19/12	212/71	44/18	Alive/6
2	77	F	< 5	1200	< 5	40/15	156/125	33/34	Alive/28
3	74	F	< 5	590	270	50/29	274/302	34/29	Alive/28

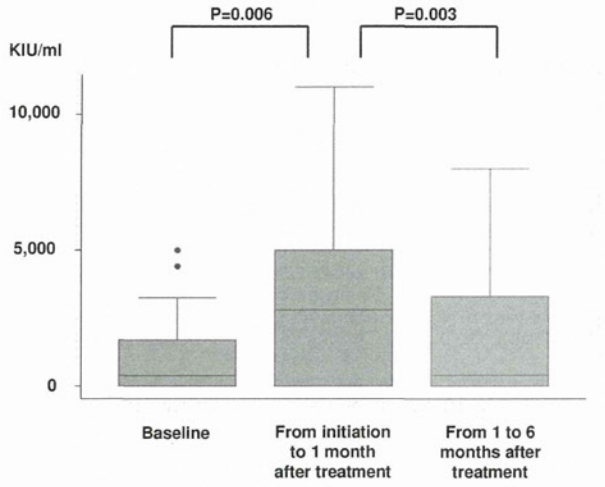

Figure 3. HCV-RNA levels at 3 points were available in 34 patients; pretreatment level, highest levels from initiation of treatment to 1 month after completing treatment, and from 1 to 6 months after treatment. HCV-RNA significantly increased during immunochemotherapy ($P = .006$) and then decreased after treatment ($P = .003$).

Although we believe that our data provide novel information about rituximab-treated patients who are HCV-positive with DLBCL, some limitations of these findings should be discussed. First, because this retrospective study included enrollment from many institutions, unrecognized biases might have been introduced. Second, we did not register all patients who were HCV-negative during the study period, but only those who were treated over the same time period as patients who were HCV-positive at each institution. This might have caused case-selection bias. Finally, we did not define the timing of immunochemotherapy withdrawal because of hepatic toxicity as we believe that the decision to terminate immunochemotherapy must be made by the treating physician.

In conclusion, our study highlighted a high incidence of severe hepatic toxicity in patients who were HCV-positive, so hepatic function should be carefully monitored in patients who are HCV-positive and receive immunochemotherapy. Well-designed studies will be necessary to determine whether early detection and prevention of HCV replication would provide improved disease management for HCV infected patients receiving immunochemotherapy.

Acknowledgments

We thank all of the clinicians and pathologists in the participating institutes for their invaluable contributions to this multicenter study.

This study was supported by a Grant-in-Aid (21-6-3) for Cancer Research from the Ministry of Health, Labor and Welfare of Japan.

Authorship

Contribution: D.E. and Y.M. designed research, performed research, analyzed data, and wrote the paper; N.N, M.K, K.I, J.T, S.K, M.O, M.Y., and A.T. designed and performed research; Y.T, K.S, A.M, K.M, A.S, M.M., and K.S. performed research; K.M. designed research, analyzed data, and wrote the paper; and T.K and T.M. designed research and gave final approval.

Conflict-of-interest disclosure: S.K. received research funding from Chugai Pharmaceutical Co Ltd; M.Y. is a medical advisor to Chugai Pharmaceutical Co Ltd; T.K. received honoraria from Chugai Pharmaceutical Co Ltd and Zenyaku Kogyo Co Ltd, and research funding from Zenyaku Kogyo Co Ltd. The remaining authors declare no competing financial interests.

Correspondence: Daisuke Ennishi, MD, Department of Hematology and Oncology, Okayama University Graduate School of Medicine, Dentistry and Pharmaceutical Science, 2-5-1 Shikata-cho, Okayama City, Okayama 700-8558, Japan; e-mail: daisukeennishi@yahoo.co.jp.

References

1. Mele A, Pulsoni A, Bianco E, et al. Hepatitis C virus and B-cell non-Hodgkin lymphomas: an Italian multicenter case-control study. *Blood.* 2003; 102(3):996-999.
2. Dolcetti R, Zancai P, De Re V, et al. Epstein-Barr virus strains with latent membrane protein-1 deletions: prevalence in the Italian population and high association with human immunodeficiency virus-related Hodgkin's disease. *Blood.* 1997; 89(5):1723-1731.
3. De Vita S, Sacco C, Sansonno D, et al. Characterization of overt B-cell lymphomas in patients with hepatitis C virus infection. *Blood.* 1997;90(2): 776-782.
4. Pioltelli P, Zehender G, Monti G, Monteverde A, Galli M. HCV and non-Hodgkin lymphoma. *Lancet.* 1996;347(9001):624-625.
5. Matsuo K, Kusano A, Sugumar A, Nakamura S, Tajima K, Mueller NE. Effect of hepatitis C virus infection on the risk of non-Hodgkin's lymphoma: a meta-analysis of epidemiological studies. *Cancer Sci.* 2004;95(9):745-752.
6. Gisbert JP, Garcia-Buey L, Pajares JM, Moreno-Otero R. Prevalence of hepatitis C virus infection in B-cell non-Hodgkin's lymphoma: systematic review and meta-analysis. *Gastroenterology.* 2003; 125(6):1723-1732.
7. Izumi T, Sasaki R, Tsunoda S, Akutsu M, Okamoto H, Miura Y. B cell malignancy and hepatitis C virus infection. *Leukemia.* 1997;11(suppl 3):516-518.
8. Luppi M, Longo G, Ferrari MG, et al. Clinico-pathological characterization of hepatitis C virus-related B-cell non-Hodgkin's lymphomas without symptomatic cryoglobulinemia. *Ann Oncol.* 1998; 9(5):495-498.
9. Besson C, Canioni D, Lepage E, et al. Characteristics and outcome of diffuse large B-cell lymphoma in hepatitis C virus-positive patients in LNH 93 and LNH 98 Groupe d'Etude des Lymphomes de l'Adulte programs. *J Clin Oncol.* 2006; 24(6):953-960.
10. Visco C, Arcaini L, Brusamolino E, et al. Distinctive natural history in hepatitis C virus positive diffuse large B-cell lymphoma: analysis of 156 patients from northern Italy. *Ann Oncol.* 2006; 17(9):1434-1440.
11. Kawatani T, Suou T, Tajima F, et al. Incidence of hepatitis virus infection and severe liver dysfunction in patients receiving chemotherapy for hematologic malignancies. *Eur J Haematol.* 2001;67(1): 45-50.
12. TIN-HsLPF P. a predictive model for aggressive non-Hodgkin's lymphoma. The International Non-Hodgkin's Lymphoma Prognostic Factors Project. *N Engl J Med.* 1993;329:987-994.
13. Coiffier B, Lepage E, Briere J, et al. CHOP chemotherapy plus rituximab compared with CHOP alone in elderly patients with diffuse large-B-cell lymphoma. *N Engl J Med.* 2002;346(4):235-242.
14. Pfreundschuh M, Trumper L, Osterborg A, et al. CHOP-like chemotherapy plus rituximab versus CHOP-like chemotherapy alone in young patients with good-prognosis diffuse large-B-cell lymphoma: a randomised controlled trial by the MabThera International Trial (MInT) Group. *Lancet Oncol.* 2006;7(5):379-391.
15. Nishimori H, Matsuo K, Maeda Y, et al. The effect of adding rituximab to CHOP-based therapy on clinical outcomes for Japanese patients with diffuse large B-cell lymphoma: a propensity score matching analysis. *Int J Hematol.* 2009;89(3): 326-331.
16. Sehn LH, Berry B, Chhanabhai M, et al. The revised International Prognostic Index (R-IPI) is a better predictor of outcome than the standard IPI for patients with diffuse large B-cell lymphoma treated with R-CHOP. *Blood.* 2007;109(5):1857-1861.
17. Winter JN, Weller EA, Horning SJ, et al. Prognostic significance of Bcl-6 protein expression in DLBCL treated with CHOP or R-CHOP: a prospective correlative study. *Blood.* 2006;107(11): 4207-4213.
18. Nyman H, Adde M, Karjalainen-Lindsberg ML, et al. Prognostic impact of immunohistochemically

defined germinal center phenotype in diffuse large B-cell lymphoma patients treated with immunochemotherapy. *Blood.* 2007;109(11):4930-4935.

19. Tsutsumi Y, Kanamori H, Mori A, et al. Reactivation of hepatitis B virus with rituximab. *Expert Opin Drug Saf.* 2005;4(3):599-608.
20. Dai MS, Chao TY, Kao WY, Shyu RY, Liu TM. Delayed hepatitis B virus reactivation after cessation of preemptive lamivudine in lymphoma patients treated with rituximab plus CHOP. *Ann Hematol.* 2004;83(12):769-774.
21. Harris NL, Jaffe ES, Diebold J, et al. World Health Organization classification of neoplastic diseases of the hematopoietic and lymphoid tissues: report of the Clinical Advisory Committee meeting-Airlie House, Virginia, November 1997. *J Clin Oncol.* 1999;17(12):3835-3849.
22. Cheson BD, Horning SJ, Coiffier B, et al. Report of an international workshop to standardize response criteria for non-Hodgkin's lymphomas. NCI Sponsored International Working Group. *J Clin Oncol.* 1999;17(4):1244.
23. Cheson BD, Pfistner B, Juweid ME, et al. Revised response criteria for malignant lymphoma. *J Clin Oncol.* 2007;25(5):579-586.
24. Markovic S, Drozina G, Vovk M, Fidler-Jenko M. Reactivation of hepatitis B but not hepatitis C in patients with malignant lymphoma and immunosuppressive therapy. A prospective study in 305 patients. *Hepatogastroenterology.* 1999;46(29):2925-2930.
25. Zuckerman E, Zuckerman T, Douer D, Qian D, Levine AM. Liver dysfunction in patients infected with hepatitis C virus undergoing chemotherapy for hematologic malignancies. *Cancer.* 1998;83(6):1224-1230.
26. Arcaini L, Merli M, Passamonti F, et al. Impact of treatment-related liver toxicity on the outcome of HCV-positive non-Hodgkin's lymphomas. *Am J Hematol.* 2010;85(1):46-50.
27. Lake-Bakaar G, Dustin L, McKeating J, Newton K, Freeman V, Frost SD. Hepatitis C virus and alanine aminotransferase kinetics following B-lymphocyte depletion with rituximab: evidence for a significant role of humoral immunity in the control of viremia in chronic HCV liver disease. *Blood.* 2007;109(2):845-846.
28. Aksoy S, Abali H, Kilickap S, Erman M, Kars A. Accelerated hepatitis C virus replication with rituximab treatment in a non-Hodgkin's lymphoma patient. *Clin Lab Haematol.* 2006;28(3):211-214.
29. Hsieh CY, Huang HH, Lin CY, et al. Rituximab-induced hepatitis C virus reactivation after spontaneous remission in diffuse large B-cell lymphoma. *J Clin Oncol.* 2008;26(15):2584-2586.
30. Hui CK, Cheung WW, Zhang HY, et al. Kinetics and risk of de novo hepatitis B infection in HBsAg-negative patients undergoing cytotoxic chemotherapy. *Gastroenterology.* 2006;131(1):59-68.
31. Yeo W, Chan TC, Leung NW, et al. Hepatitis B virus reactivation in lymphoma patients with prior resolved hepatitis B undergoing anticancer therapy with or without rituximab. *J Clin Oncol.* 2009;27(4):605-611.
32. Sumazaki R, Matsubara T, Aoki T, Nagai Y, Shibasaki M, Takita H. Rapidly progressive hepatitis C in a patient with common variable immunodeficiency. *Eur J Pediatr.* 1996;155(7):532-534.
33. Peffault de Latour R, Levy V, Asselah T, et al. Long-term outcome of hepatitis C infection after bone marrow transplantation. *Blood.* 2004;103(5):1618-1624.

blood

2012 119: 285-295
Prepublished online November 10, 2011;
doi:10.1182/blood-2011-01-332478

Synthetic retinoid Am80 ameliorates chronic graft-versus-host disease by down-regulating Th1 and Th17

Hisakazu Nishimori, Yoshinobu Maeda, Takanori Teshima, Haruko Sugiyama, Koichiro Kobayashi, Yoshiko Yamasuji, Sachiyo Kadohisa, Hidetaka Uryu, Kengo Takeuchi, Takehiro Tanaka, Tadashi Yoshino, Yoichiro Iwakura and Mitsune Tanimoto

Blood (print ISSN 0006-4971, online ISSN 1528-0020), is published weekly by the American Society of Hematology, 2021 L St, NW, Suite 900, Washington DC 20036.

Synthetic retinoid Am80 ameliorates chronic graft-versus-host disease by down-regulating Th1 and Th17

Hisakazu Nishimori,[1] Yoshinobu Maeda,[1] Takanori Teshima,[2] Haruko Sugiyama,[1] Koichiro Kobayashi,[1] Yoshiko Yamasuji,[1] Sachiyo Kadohisa,[1] Hidetaka Uryu,[2] Kengo Takeuchi,[3] Takehiro Tanaka,[4] Tadashi Yoshino,[4] Yoichiro Iwakura,[5] and Mitsune Tanimoto[1]

[1]Department of Hematology and Oncology, Okayama University Graduate School of Medicine, Dentistry, and Pharmaceutical Sciences, Okayama, Japan; [2]Center for Cellular and Molecular Medicine, Kyushu University Graduate School of Science, Fukuoka, Japan; [3]Pathology Project for Molecular Targets, Cancer Institute, Japanese Foundation for Cancer Research, Tokyo, Japan; [4]Department of Pathology, Okayama University Graduate School of Medicine, Dentistry, and Pharmaceutical Sciences, Okayama, Japan; and [5]Center for Experimental Medicine and Systems Biology, Institute of Medical Science, University of Tokyo, Tokyo, Japan

Chronic GVHD (cGVHD) is a main cause of late death and morbidity after allogeneic hematopoietic cell transplantation, but its pathogenesis remains unclear. We investigated the roles of Th subsets in cGVHD with the use of a well-defined mouse model of cGVHD. In this model, development of cGVHD was associated with up-regulated Th1, Th2, and Th17 responses. Th1 and Th2 responses were up-regulated early after BM transplantation, followed by a subsequent up-regulation of Th17 cells. Significantly greater numbers of Th17 cells were infiltrated in the lung and liver from allogeneic recipients than those from syngeneic recipients. We then evaluated the roles of Th1 and Th17 in cGVHD with the use of IFN-γ–deficient and IL-17–deficient mice as donors. Infusion of IFN-$\gamma^{-/-}$ or IL-$17^{-/-}$ T cells attenuated cGVHD in the skin and salivary glands. Am80, a potent synthetic retinoid, regulated both Th1 and Th17 responses as well as TGF-β expression in the skin, resulting in an attenuation of cutaneous cGVHD. These results suggest that Th1 and Th17 contribute to the development of cGVHD and that targeting Th1 and Th17 may therefore represent a promising therapeutic strategy for preventing and treating cGVHD. (*Blood.* 2012; 119(1):285-295)

Introduction

GVHD is a result of immune attack of host tissues, such as the skin, gut, liver, and lung, by donor T cells in transplants.[1,2] On the basis of the differences in clinical manifestations and histopathology, GVHD can be divided into acute and chronic types. Chronic GVHD (cGVHD) is the main cause of late death and morbidity after allogeneic hematopoietic stem cell transplantation.[3-5] cGVHD often presents with clinical manifestations that resemble those observed in autoimmune diseases, such as systemic lupus erythematosus, Sjögren syndrome, lichen planus, and scleroderma. It has traditionally been assumed that the predominant cytokines produced during acute GVHD are Th1 cytokines, whereas those produced during cGVHD are Th2 cytokines. Although recent studies have suggested that cGVHD could be caused by cytokines secreted by Th1 cells,[6] Th17 cells,[7] or autoantibodies,[8] or both, the immune mechanisms leading to the development of cGVHD are not completely understood.

Th17 cells are a third subset of polarized effector T cells characterized by their expression of proinflammatory cytokine IL-17 and other cytokines.[9] IL-17 belongs to a family of 6 members: IL-17A, IL-17B, IL-17C, IL-17D, IL-17E (also known as IL-25), and IL-17F. Of these, IL-17A and IL-17F are the best characterized cytokines and form heterodimers. IL-17 plays an important role in the control and clearance of various pathogens.[9] In addition, Th17 cells have been implicated in allograft rejection of solid organs and several autoimmune diseases.[10,11] Although a number of studies have addressed how Th17 cells contribute to GVHD[12] and have reported that Th17 cells are sufficient but not necessary to induce acute GVHD,[13,14] the functional role of Th17 in cGVHD is unclear.

Retinoic acid, the active metabolite of vitamin A, has multiple effects on cell differentiation and survival by ligating the receptors from 2 families, retinoic acid receptors (RARs) and retinoid X receptors, each of which exists in multiple isoforms.[15] All-*trans*-retinoic acid (ATRA) has been reported to inhibit IFN-γ synthesis by Thl cells and to suppress the differentiation of Th17 cells by down-regulating the orphan nuclear receptor RORγt, a key regulator of Th17 differentiation.[16-19] Am80 is a novel RARα/β-specific synthetic retinoid that shows ~ 10-fold more potent biologic activity than ATRA by binding to RARα and RARβ but not to RARγ.[20] Am80 also inhibits IL-6 signaling[20,21] and reduces the severity and progression of inflammatory disease models.[20-23]

In the present study, we used the B10.D2 ($H\text{-}2^d$) into BALB/c ($H\text{-}2^d$) MHC-compatible, multiple minor histocompatibility Ag (miHA)–incompatible model of cGVHD to address the contribution of Th1/Th17 cells and the effects of retinoids on cGVHD with the use of IFN-$\gamma^{-/-}$ mice and IL-$17^{-/-}$ mice as donors. We also tested the hypothesis that the administration of Am80 ameliorates cGVHD by reducing the levels of Th1 and Th17 inflammatory cytokines and the fibrosis factor TGF-β.

Submitted January 26, 2011; accepted October 29, 2011. Prepublished online as *Blood* First Edition paper, November 10, 2011; DOI 10.1182/blood-2011-01-332478.

The online version of this article contains a data supplement.

The publication costs of this article were defrayed in part by page charge payment. Therefore, and solely to indicate this fact, this article is hereby marked "advertisement" in accordance with 18 USC section 1734.

Methods

Mice

Female B10.D2 (H-2^d) mice were purchased from Japan SLC. BALB/c (H-2^d) recipient mice were purchased from Charles River Japan. IL-17A–deficient (IL-17$^{-/-}$) mice with the BALB/c background were generated previously.[24] IFN-γ–deficient (IFN-γ$^{-/-}$) mice were purchased from The Jackson Laboratory. IL-17$^{-/-}$ and IFN-γ$^{-/-}$ mice with the B10.D2 background were backcrossed for 8-10 generations from the original knockout mice. All experiments involving animals were performed according to the regulations of the Institutional Animal Care and Research Advisory Committee, Okayama University Advanced Science Research Center.

BM transplantation

Mice received transplants according to the standard protocols described previously.[25] Briefly, BALB/c mice received a single dose of 6.75 Gy x-ray total body irradiation. Recipient mice were injected with 2×10^6 spleen T cells and 8×10^6 T cell–depleted BM (TCD-BM) cells from B10.D2 donors. T-cell depletion and purification were performed with anti-CD90.2 Microbeads, pan T-cell isolation kit, and CD25 isolation kit and an AutoMACS system (Miltenyi Biotec) according to the manufacturer's instructions. Donor cells were injected intravenously into the recipients on day 0.

Evaluation of cGVHD

After BM transplantation (BMT), animals were weighed every 3 days and scored for skin manifestations of GVHD. The following scoring system was used[25]: healthy appearance, 0; skin lesions with alopecia < 1 cm^2 in area, 1; skin lesions with alopecia 1-2 cm^2 in area, 2; skin lesions with alopecia > 2 cm^2 in area, 3. In addition, animals were assigned 0.3 points each for skin disease (lesions or scaling) on the ears, tails, and paws. The minimum score was 0, and the maximum score was 3.9.

Tissue histopathology

Shaved skin from the interscapular region (~ 2 cm^2), the left lung, liver, and colon specimens of recipients were fixed in 10% formalin, embedded in paraffin, sectioned, mounted on slides, and stained with H&E. Slides were scored by a pathologist blind to experimental group (K.T.) on the basis of dermal fibrosis, fat loss, inflammation, epidermal interface changes, and follicular drop-out (0-2 for each category; the maximum score was 10).[25] Lung, liver, and colon slides were scored by a pathologist blind to the experimental group (T.T.). Lung slides were scored according to periluminal infiltrates, pneumonitis, and the extent of injury (0-3 for each category), and the maximum score was 9.[26] Liver slides were scored according to bile duct injury and inflammation (0-4 for each category), and the maximum score was 8.[27] Colon slides were scored according to crypt apoptosis and inflammation (0-4 for each category), and the maximum score was 8.[27]

Intracellular cytokine staining and cytokine analysis

Organs from mice were removed, processed into single-cell suspensions, and stimulated in vitro with 50 ng/mL phorbol 12-myristate 13-acetate (PMA; Sigma-Aldrich) and 100 ng/mL ionomycin (Sigma-Aldrich) at 37°C for 3 hours. Cells were then incubated with GolgiStop (BD PharMingen) for an additional 2 hours. mAbs conjugated to fluorescein isothiocyanate, phycoerythrin, peridinin-chlorophyll protein complexes, allophycocyanin, or Alexa Fluor 488 were used to assess the cell populations and were purchased from BD PharMingen or eBioscience. Cells were analyzed on a FACSCalibur flow cytometer with CellQuest software (both from Becton Dickinson) or MACS Quant flow cytometer (Miltenyi Biotec) with FlowJo software (TreeStar); both were housed in the Central Research Laboratory, Okayama University Medical School. Total peripheral lymph node (PLN) cells were adjusted to 1×10^6/mL in cultures. Supernatants were removed, and cytokine levels were measured with a BD Cytometric Bead Array (CBA) or by ELISA (R&D Systems) according to the respective manufacturer's protocol.

IFN-γ neutralization

Anti–mouse IFN-γ mAbs for in vivo experiments were prepared from mouse ascites from clones R4-6A2. Mice were treated intraperitoneally with anti–IFN-γ mAbs or rat IgG (160 μg/mouse; Sigma-Aldrich) on days 0, 5, 10, and 15 after BMT.

Administration of ATRA and Am80

Recipients were orally administered ATRA (200 μg/mouse; Wako), Am80 (1.0 mg/kg body weight; Nippon Shinyaku), or vehicle solutions daily from day 0.

Real-time RT-PCR

Total RNA was isolated from homogenized ear tissue with the use of an RNeasy mini kit (QIAGEN). cDNA synthesis was initiated by application of oligo dT primers and TaqMan Reverse Transcription Reagents (Applied Biosystems). Target cDNA levels were quantified by real-time PCR. The TaqMan Universal PCR Master Mix and the following Assay-on-Demand mouse gene-specific fluorescently labeled TaqMan MGB probes were used in an ABI Prism 5300 sequence detection system (Applied Biosystems): Mm01178820_m1 (TGF-β1). The mRNA expression of individual genes was normalized relative to GAPDH with the use of the equation $dCt = Ct_{target} - Ct_{GAPDH}$. The samples were obtained at room temperature using light microscopy (BX51; Olympus) with an objective lens (10×/0.40 NA, or 20×/0.70 NA; Olympus) and a camera (DP-70; Olympus). The images were acquired with image processing software (DP2-BSW Version 1.2; Olympus).

Statistical analyses

Group comparisons of skin cGVHD scores and pathology scores were performed using the Mann-Whitney U test or Kruskal-Wallis test. Cell populations, cytokine levels, mean weights, and gene expression data were analyzed with the unpaired 2-tailed Student t test. In all analyses, $P < .05$ was taken to indicate statistical significance.

Results

Th17 cells are increased in lymphoid organs during cGVHD development

We first assessed the kinetics of Th1/Th2/Th17 cytokine production of donor T cells generated during cGVHD. We used the most common cGVHD model: the MHC-compatible, multiple miHA-incompatible allogeneic BMT model (B10.D2 into BALB/c). Sublethally irradiated (6.75 Gy) BALB/c mice were transplanted with 2×10^6 B10.D2 spleen T cells and 8×10^6 B10.D2 TCD-BM cells. Ly9.1 was used as a marker to distinguish donors from recipients; B10.D2 and BALB/c are negative and positive for Ly9.1, respectively. Flow cytometric analysis of the spleens and PLNs on days 14 and 28 indicated that donor chimerism as determined by the negativity for Ly9.1 was $> 95\%$. The allogeneic recipients showed pathologic damage to the skin, salivary glands, lung, and liver, as reported previously (Figure 1A).[25,27] Cells isolated from PLNs were harvested on days 14 and 28 after BMT and analyzed for cytokine expression. In the early phase (day 14), IL-17$^+$ T cells were detected more frequently in the PLNs of recipients of syngeneic BMT, whereas in the late phase (day 28), IL-17$^+$ T cells in allogeneic recipients increased and were detected significantly more frequently than in syngeneic recipients (Figure 1B). We detected consistently higher percentages of donor T cells expressing IFN-γ and IL-13 in PLNs from allogeneic recipients than from syngeneic recipients (Figure 1B). Intracellular staining showed that most of the IL-17–producing cells were CD4$^+$ T cells (Figure 1C) and that IFN-γ/IL-17 double-positive cells (Th1/Th17

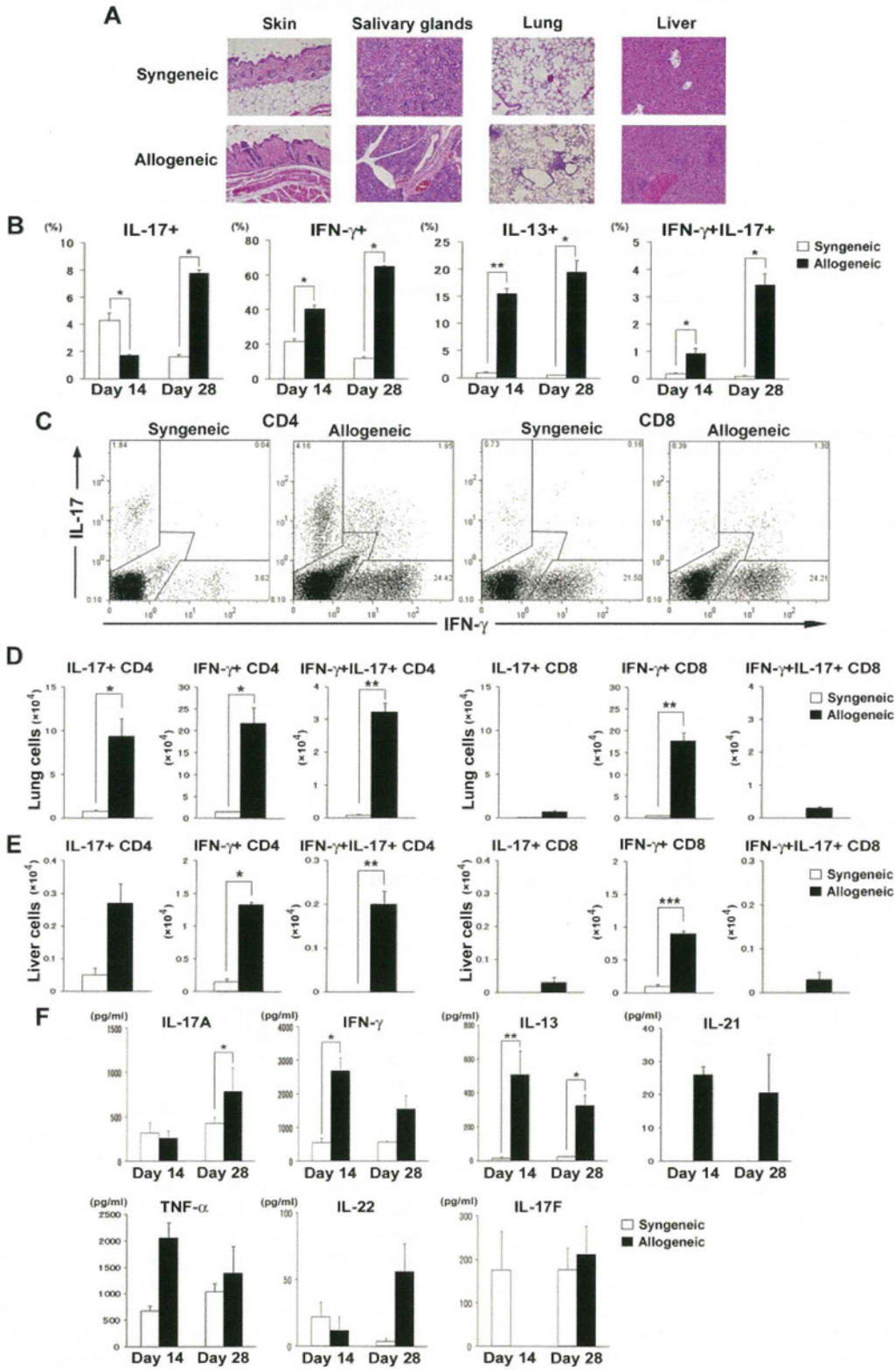

Figure 1. Th17 cells are increased in lymphoid organs during the late phase of cGVHD. Sublethally irradiated (6.75 Gy) BALB/c mice were transplanted with 2×10^6 spleen T cells plus 8×10^6 TCD-BM from WT B10.D2 mice (allogeneic group; black bars). The syngeneic group (white bars) received a transplant of the same dose of splenocytes and TCD-BM from BALB/c mice. (A) Histopathology of skin, salivary glands, lung, and liver of syngeneic and allogeneic recipients 35 days after BMT. (B) The percentages of donor-derived $CD3^+$ T cells expressing IL-17, IFN-γ, IL-13, and IFN-γ/IL-17 on days 14 and 28 are shown. (C) Representative staining for intracellular IFN-γ and IL-17 on $CD4^+$ and $CD8^+$ T cells on day 28 for syngeneic and allogeneic mice. (D-E) Absolute numbers of IL-17–, IFN-γ–, and IFN-γ/IL-17–producing $CD4^+$ and $CD8^+$ T cells in recipient lung (D) and liver (E). (F) PLN cells from syngeneic and allogeneic recipients on days 14 and 28 were stimulated with PMA and ionomycin in vitro. Five hours later, the supernatants were collected to determine cytokine levels by ELISA or CBA. Graphs indicate the levels of cytokines secreted per 1×10^6 total stimulated PLN cells. Three to 6 mice per group were used. The means (± SE) of each group are shown. Data are from 1 representative of ≥ 2 independent experiments. $^*P < .05$, $^{**}P < .01$, and $^{***}P < .005$.

cells) were exclusively detected in allogeneic recipients (Figure 1B-C). As allogeneic recipients developed GVHD-induced lymphopenia on day 28; absolute numbers of IFN-γ^+ T and IL-17^+ T cells in PLNs from allogeneic recipients were not greater than those from syngeneic recipients (IFN-γ^+ T, $51.8 \pm 17.5 \times 10^4$ vs $49.4 \pm 4.2 \times 10^4$, $P = .92$; IL-17^+ T, $5.9 \pm 2.2 \times 10^4$ vs $6.9 \pm 0.59 \times 10^4$, $P = .16$). Numbers of Th1 and Th17 cells from allogeneic recipients were significantly greater than those from syngeneic recipients in the lung (Figure 1D) and liver (Figure 1E). Cells isolated from PLNs of allogeneic recipients secreted significantly greater amounts of IL-17, IFN-γ, and IL-13 after stimulation with PMA and ionomycin (Figure 1F) or without stimulation (supplemental Figure 1, available on the *Blood* Web site; see the Supplemental Materials link at the top of the online article). These cytokine levels were also elevated in serum from allogeneic recipients 28 days after BMT (supplemental Figure 2). To confirm that our observations were not strain dependent or model dependent, we performed similar experiments in the DBA/2 into BALB/c model of cGVHD. We confirmed the up-regulated Th1 and Th17 responses in this model (supplemental Figure 3).

IL-$17^{-/-}$ donor T cells ameliorate cGVHD

We next used IL-$17^{-/-}$ mice with the B10.D2 background as donors to evaluate whether Th17 contributes to cGVHD. On transfer of IL-$17^{-/-}$ B10.D2 donor T cells into allogeneic BMT models, weight loss was mild and fur loss was clearly ameliorated in comparison to that seen in recipients of wild-type (WT) T cells (Figure 2A-B). Clinical cGVHD severity was assessed with a standard scoring system (see "Methods"). Allogeneic IL-$17^{-/-}$ BMT recipients showed significantly less skin cGVHD than WT controls ($P < .05$; Figure 2C). Histopathologic examination of the skin showed significantly reduced cGVHD pathology in recipients of IL-$17^{-/-}$ donors (3.17 ± 1.09 vs 8.50 ± 0.84; $P < .01$; Figure 2D). A dry mouth is one of the distinctive features of cGVHD, and lymphocytic inflammation, fibrosis, and atrophy of acinar tissue were observed in the salivary glands of WT BMT recipients. Histopathologic examination of the salivary glands showed reduced cGVHD pathology in the recipients of IL-$17^{-/-}$ donors (Figure 2E). Atrophy of the salivary glands as determined by their size was significantly reduced in recipients of IL-$17^{-/-}$ donors (4.21 ± 0.13 vs 3.54 ± 0.11; $P < .01$; Figure 2E). No significant differences were observed in pathology scores of the lung, liver, or colon between recipients of IL-$17^{-/-}$ and WT donors (lung, 2.6 ± 1.04 vs 0.8 ± 0.44, $P = .19$; liver, 1.5 ± 0.87 vs 1.83 ± 0.37, $P = .75$; colon, 1.6 ± 0.36 vs 2.8 ± 0.33, $P = .06$). Thus, IL-$17^{-/-}$ BMT recipients showed less cGVHD in the skin and salivary glands than did the WT controls. Flow cytometric analysis of the PLNs in the early phase (day 14) showed no differences in frequency of IFN-g^+ cells between IL-$17^{-/-}$ and WT recipients, whereas recipients of IL-$17^{-/-}$ showed fewer IFN-γ^+ cells in the late phase (day 35, $4.3\% \pm 0.8\%$ vs $18.9\% \pm 3.5\%$; $P = .01$; Figure 2F). As allogeneic WT recipients developed more severe GVHD-induced lymphopenia on day 35 than IL-$17^{-/-}$ recipients, absolute numbers of IFN-g^+ cells in PLNs from allogeneic WT recipients were not greater than those from IL-$17^{-/-}$ recipients (IFN-γ^+ T cells, $6.08 \pm 0.87 \times 10^4$ vs $4.83 \pm 1.23 \times 10^4$; $P = .48$). As expected, IFN-γ/IL-17 double-positive cells were not detected in recipients of IL-$17^{-/-}$ donors on days 14 and 35 (Figure 2G-H). No differences were observed in the IL-13^+ cells or Foxp3^+ cells between the groups (data not shown). These data suggest that donor IL-17 contributes to the pathogenesis of cGVHD.

Donor Th1 differentiation is responsible for the development of cGVHD

To test whether donor Th1 differentiation is responsible for cGVHD, we used IFN-$\gamma^{-/-}$ mice with the B10.D2 background as donors. BMT from IFN-$\gamma^{-/-}$ donors compared with WT donors significantly improved the clinical cGVHD score ($P < .05$; Figure 3A). Histopathologic examination of the skin showed significantly reduced cGVHD pathology in recipients of IFN-$\gamma^{-/-}$ donors (4.75 ± 0.54 vs 7.80 ± 0.52; $P = .02$; Figure 3B). Salivary gland atrophy was also reduced in recipients of IFN-$\gamma^{-/-}$ donors (3.81 ± 0.05 vs 2.87 ± 0.19; $P < .05$; Figure 3C). No significant differences were observed in pathology scores of the lung, liver, or colon between recipients of IFN-$\gamma^{-/-}$ and WT donors (lung, 2.4 ± 0.61 vs 3.2 ± 0.52, $P = .4$; Figure 3B; liver, 1.0 ± 0.4 vs 1.6 ± 0.32, $P = .21$; colon, 0.75 ± 0.21 vs 1.6 ± 0.67, $P = .36$). Intracellular staining of PLNs showed no differences in IL-13– or IL-17–producing cells between IFN-$\gamma^{-/-}$ and WT recipients (data not shown), although significantly greater numbers of Foxp3^+ cells were detected in the IFN-$\gamma^{-/-}$ recipients (day 35; $P < .05$; Figure 3D). To examine whether an increase in numbers of Treg cells was responsible for the reduced cGVHD in the absence of donor IFN-$\gamma^{-/-}$, mice were injected with whole T cells or CD25-depleted T cells from donors. As shown in Figure 3E, depletion of CD25^+ cells from the donor inoculum exacerbated skin scores ($P < .05$). However, CD25-depleted T cells from IFN-$\gamma^{-/-}$ mice caused less severe skin GVHD than those from WT mice ($P < .05$). These findings suggest that IFN-γ contributes to the pathogenesis of cGVHD by both Treg-independent and -dependent pathways. Next, we evaluated the role of IFN-γ in the development of skin cGVHD by administering anti–IFN-γ mAbs to recipients of WT or IL-$17^{-/-}$ donors. Anti–IFN-γ mAb treatment significantly reduced skin scores and pathology scores in recipients of WT donors (Figure 3F-G). Recipients of IL-$17^{-/-}$ donors again showed reduced skin scores, and treatment with anti–IFN-γ mAbs further reduced skin scores (Figure 3H). These findings suggest that IFN-γ contributes to cGVHD pathogenesis.

Am80 inhibits donor Th1 and Th17 cells both in vitro and in vivo

ATRA has been reported to suppress the differentiation of Th17 cells with a reciprocal induction of Treg cells.[28] Am80, a novel RARα/β-specific synthetic retinoid, has a biologic activity ~ 10 times more potent than that of ATRA[20] and directly inhibits Th1 cytokine production.[20,22,29] Therefore, we hypothesized that ATRA or Am80 down-regulates both Th1 and Th17 differentiation in donor T cells, resulting in attenuation of cGVHD. To clarify whether retinoids directly inhibit the production of cytokines, PLNs were isolated from mice 14 days after allogeneic BMT and cultured with Am80 for 24 hours to determine cytokine production. Am80 inhibited IFN-γ (Figure 4A) and IL-17 (Figure 4B) production in a dose-dependent manner. Next, BMT recipients were orally administered Am80 at a dose of 1.0 mg/kg of body weight or vehicle daily from day 0 of BMT, and cytokine expression was assessed in PLNs harvested on day 35. We detected significantly fewer IFN-γ^+ T cells in Am80-administered recipients (Figure 4C). In addition, PLNs from Am80-treated recipients produced significantly less IFN-γ after stimulation with PMA and ionomycin ($P < .01$; Figure 4D). No difference was observed in the percentage of IL-17–producing donor cells, although PLN cells from Am80-treated recipients produced significantly less IL-17 ($P < .05$) and IL-21 ($P < .01$) after stimulation with PMA and ionomycin (Figure 4D). Taken together, these data suggest that Am80 down-regulates both Th1 and Th17 cells in vitro and in vivo.

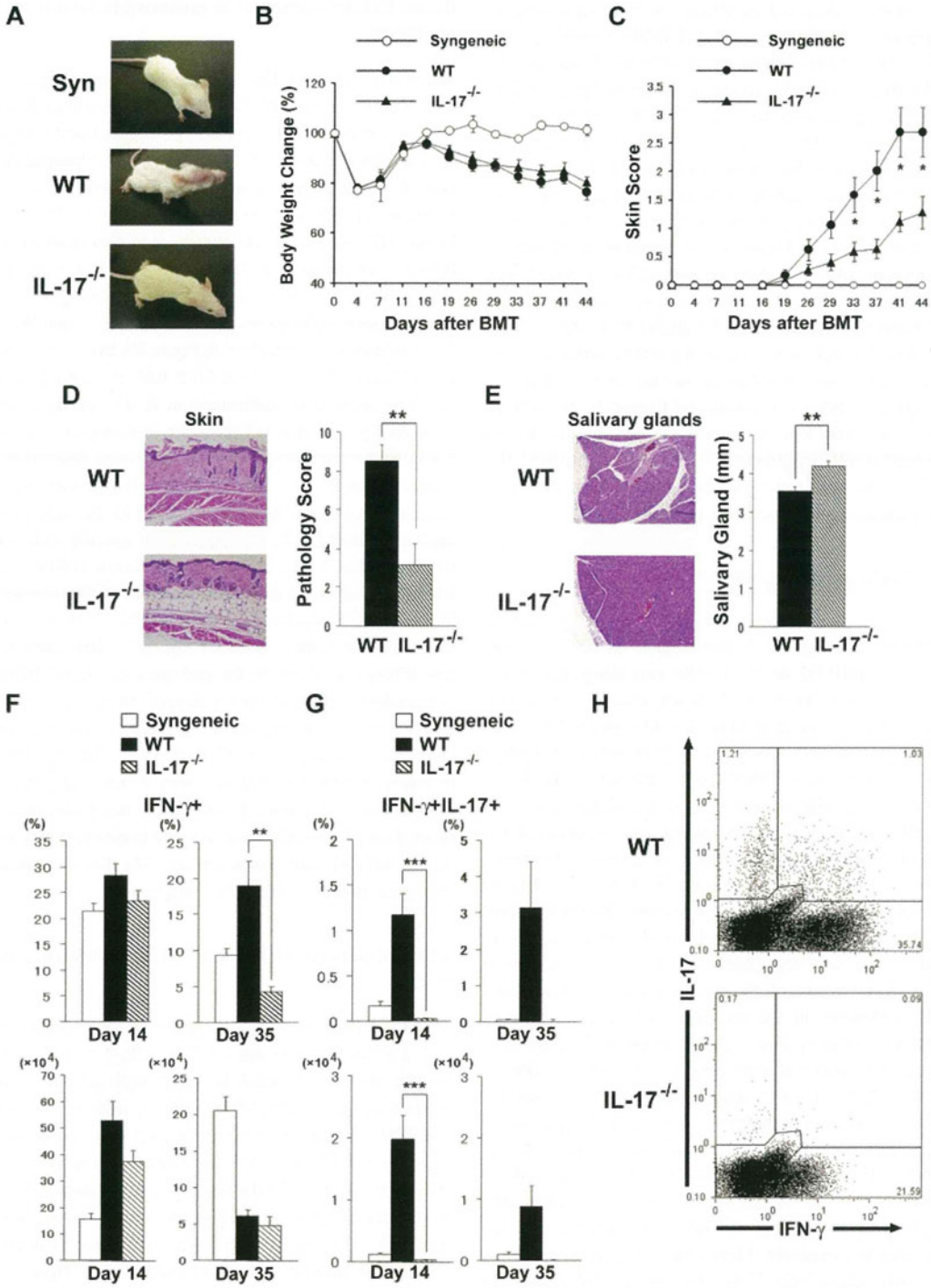

Figure 2. IL-17$^{-/-}$ donor T cells ameliorate cGVHD. Sublethally irradiated BALB/c recipients were transplanted from WT, IL-17$^{-/-}$ B10.D2, or syngeneic BALB/c donors. (A) Gross observation of the skin lesions from recipients of syngeneic, WT, and IL-17$^{-/-}$ donors 28 days after BMT. The recipients were analyzed for body weight (B) and cGVHD skin scores (C); data from 2 independent experiments were combined (n = 14 per group). Pathology score of skin (D) and the longest diameter of the salivary gland (E) on day 35 of BMT are shown. Four to 6 recipients were examined in each group. (F-G) PLN cells of the recipients of syngeneic (white bar), WT (black bar), or IL-17$^{-/-}$ (striped bar) donors were stained for intracellular IFN-γ and IL-17 on days 14 and 35 after BMT. The percentages and absolute numbers of IFN-γ$^+$ cells (F) and IFN-γ$^+$/IL-17$^+$ cells (G) are shown. Data from 2 replicated experiments were combined (n = 6-11 per group). (H) Representative staining for intracellular IFN-γ and IL-17 on CD4$^+$ T cells of WT or IL-17$^{-/-}$ mice on day 35 is shown. Data represent the means ± SEs. *$P \leq .05$, **$P \leq .01$, and ***$P \leq .001$.

Administration of Am80 ameliorates cGVHD

Next, we examined whether ATRA or Am80 can down-regulate cGVHD. BALB/c recipients were orally administered ATRA (200 μg/mouse) or Am80 from day 0 of BMT. We found that ATRA tended to decrease the clinical cGVHD score (Figure 5A), whereas Am80 significantly ameliorated the clinical score compared with controls ($P = .01$; Figure 5B). Histopathologic examination of the skin on day 16 showed significantly reduced cGVHD damage in Am80-treated animals (day 16, 4.8 ± 0.4 vs 7.4 ± 0.4; $P < .01$; Figure 5C), No differences were observed in pathology scores of the lung, liver, or colon between the 2 groups (Figure 5C). Because it has been reported that Am80 can induce Treg cells,[29] we

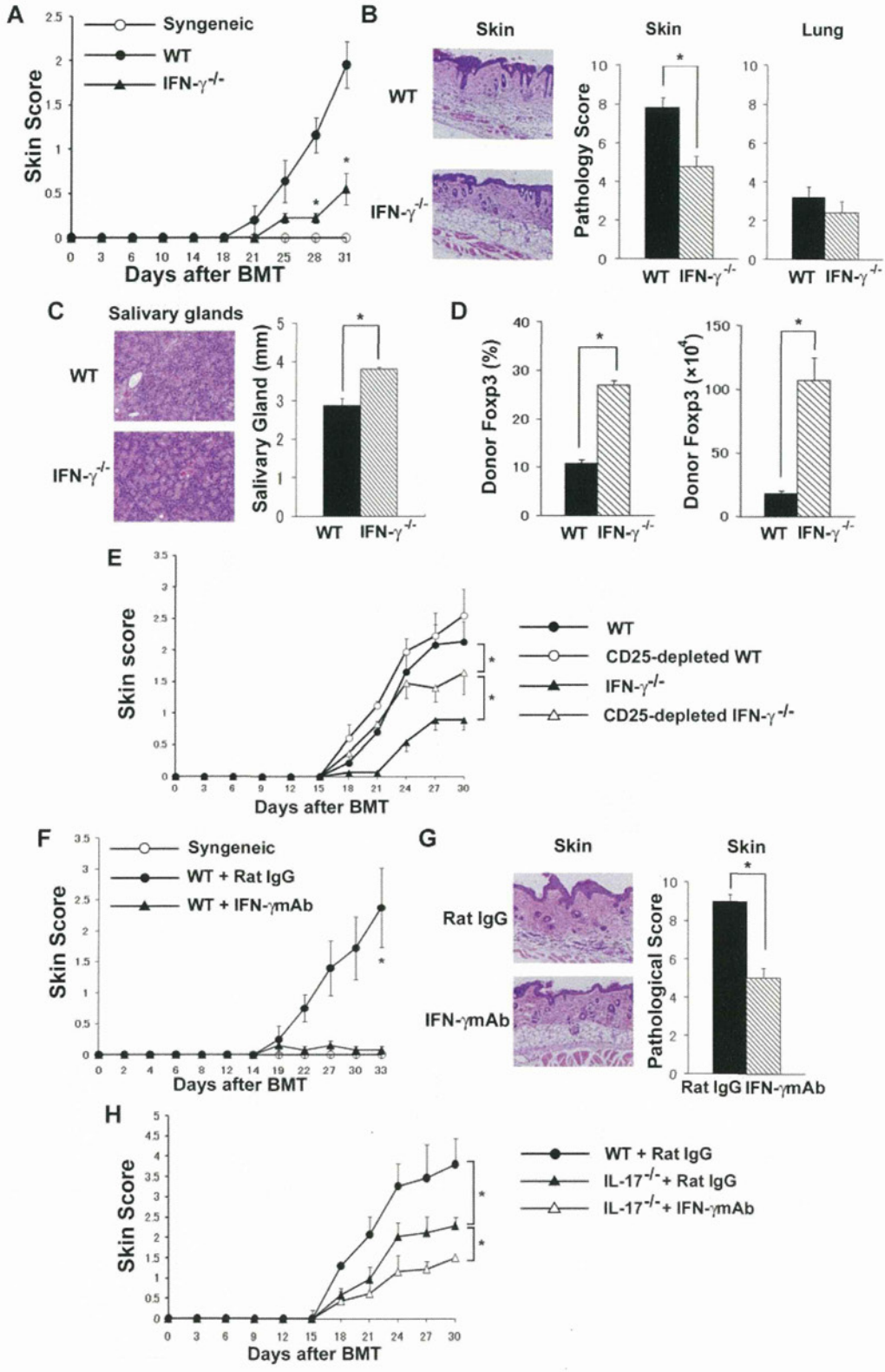

Figure 3. Donor Th1 differentiation and IFN-γ production are responsible for exacerbated cGVHD. (A-D) Sublethally irradiated BALB/c recipients were transplanted from WT or IFN-$\gamma^{-/-}$ B10.D2 donors. Clinical skin cGVHD scores (A), pathology score of skin and lung (B), and the longest diameter of the salivary gland (C) on day 35 after BMT are shown. Four to 6 recipients were examined in each group. Data are from 1 representative of 3 independent experiments. (D) PLN cells of the recipients on day 35 were stained for intracellular Foxp3. The percentages and the absolute number of $CD4^+Foxp3^+$ Treg cells are shown. Four to 6 recipients were examined in each group. Data are from 1 representative of 2 independent experiments. (E) Sublethally irradiated BALB/c recipients were transplanted 8×10^6 TCD-BM cells plus 2×10^6 total spleen T cells or CD25-depleted T cells from WT or IFN-$\gamma^{-/-}$ B10.D2 donors. The skin cGVHD scores are shown ($n = 6$ per group). Data are from 1 representative of ≥ 2 independent experiments. (F-H) Sublethally irradiated BALB/c recipients were transplanted from WT or IL-$17^{-/-}$ B10.D2 donors. The recipients were injected with anti–IFN-γ mAbs or rat IgG (160 μg/mouse) on days 0, 5, 10, and 15 after BMT and were assessed for the clinical signs of cGVHD every 3 days. The clinical skin cGVHD scores (F), histopathology, and pathology score of the skin (G) on day 35 of BMT from WT donors. Four mice per group were used. Data are from 1 representative of ≥ 2 repeated experiments. (H) The clinical skin cGVHD scores after BMT from WT or IL-$17^{-/-}$ donors are shown. Six mice per group were used. Data are from 1 representative of 2 independent experiments. The means (± SEs) of each group are shown; *$P < .05$.

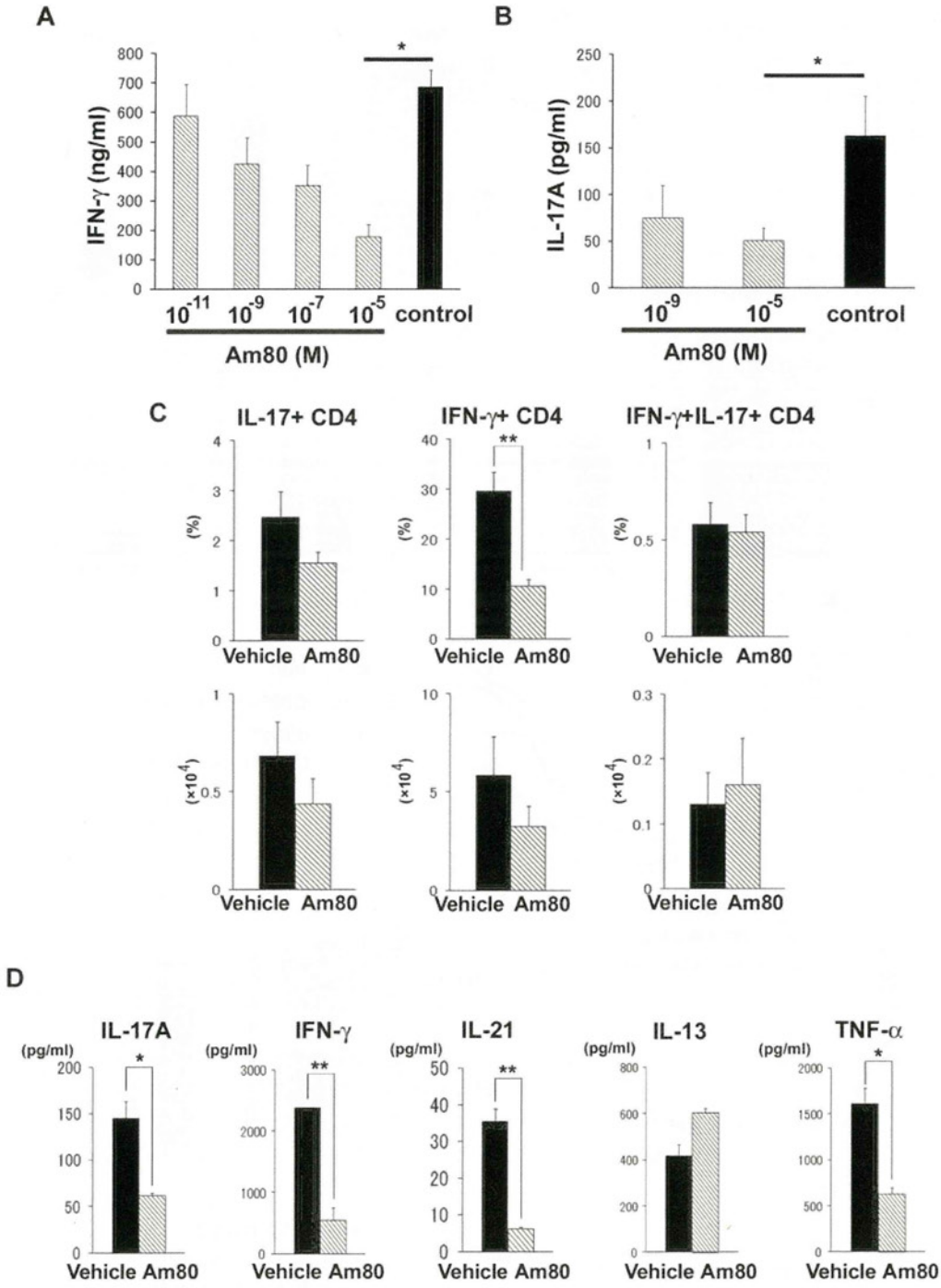

Figure 4. Am80 inhibits donor Th1 and Th17 cells in vitro and in vivo. Sublethally irradiated BALB/c recipients were transplanted from WT B10.D2 donors. (A-B) PLN cells from recipients (n = 3-6 per group) on day 14 were treated with Am80 or vehicle solution for 24 hours, the supernatants were collected, and ELISA was performed to determine the cytokine levels. Graphs represent the levels of cytokines secreted per 1×10^6 whole stimulated PLN cells. The data are from 1 representative of ≥ 3 independent experiments. (C-D) After BMT, recipients (n = 4-6 per group) were administered oral Am80 (1.0 mg/kg of body weight) or vehicle solution daily from day 0. PLNs of the recipients were stained for intracellular IFN-γ and IL-17. (C) The percentage and absolute number of IFN-γ$^+$ and IL-17$^+$–producing CD4$^+$ T cells. Data are from 1 representative of ≥ 2 repeated experiments. (D) PLN cells from recipients (n = 3-6 per group) treated with Am80 or vehicle on day 16 were stimulated with PMA and ionomycin. Five hours later, the supernatants were collected to determine cytokine levels by CBA. Graphs represent the levels of cytokines secreted per 1×10^6 whole stimulated PLN cells. The data are from 1 representative of ≥ 3 independent experiments. The means (± SEs) of each group are shown; $^*P < .05$ and $^{**}P < .01$.

quantified the frequency of Foxp3-expressing CD4$^+$ T cells in the PLNs after BMT. Recipients administered Am80 showed a decreased frequency of Foxp3$^+$ cells (day 17, 12.3% ± 2.5% vs 23.5% ± 2.6%; $P = .02$; Figure 5D). Foxp3 mRNA expression of the target organ (the ear) was also decreased in the Am80 recipients (data not shown). To confirm that the effects of Am80 are independent of Treg cells, mice were injected with whole T cells or CD25-depleted T cells from donors. As shown in Figure 5E, depletion of CD25$^+$ cells from the donor inoculum did not exacerbate skin cGVHD in Am80-treated mice, thus suggesting that the effects of Am80 treatment are not associated with Treg cells.